

1 Reanalysis of long-term series of glaciological and geodetic 2 mass balance for ten Norwegian glaciers

3 Liss M. Andreassen¹, Hallgeir Elvehøy¹, Bjarne Kjølmoen¹ and Rune V. Engeset¹

4 [1]{Section for Glaciers, Ice and Snow, the Norwegian Water Resources and Energy
5 Directorate (NVE), Oslo, Norway}

6 Correspondence to: L. M. Andreassen (lma@nve.no)

7

8 **Abstract**

9 Glaciological and geodetic methods provide independent observations of glacier mass balance.
10 The glaciological method measures the surface mass balance, on a seasonal or annual basis,
11 whereas the geodetic method measures surface, internal and basal mass balances, over a period
12 of years or decades. In this paper, we reanalyse the 10 glaciers with long-term mass balance
13 series in Norway. The reanalysis includes (i) homogenisation of both glaciological and geodetic
14 observation series, (ii) uncertainty assessment, (iii) estimates of generic differences including
15 estimates of internal and basal melt, (iv) validation, and, if needed, (v) calibration of mass
16 balance series. This study comprises an extensive set of data (484 mass balance years, 34
17 geodetic surveys and large volumes of supporting data, such as metadata and field notes).

18 In total, 21 periods of data were compared and the results show discrepancies between the
19 glaciological and geodetic methods for some glaciers, which in part are attributed to internal
20 and basal ablation and in part to inhomogeneity in the data processing. Deviations were smaller
21 than 0.2 m w.e. a⁻¹ for 12 out of 21 periods. Calibration was applied to seven out of 21 periods,
22 as the deviations were larger than the uncertainty.

23 The reanalysed glaciological series shows a more consistent signal of glacier change over the
24 period of observations than previously reported: Six glaciers had a significant mass loss (14-22
25 m w.e.) and four glaciers were nearly in balance. All glaciers have lost mass after year 2000.

26 More research is needed on the sources of uncertainty, to reduce uncertainties and adjust the
27 observation programmes accordingly. The study confirms the value of carrying out independent
28 high-quality geodetic surveys to check and correct field observations.

29 **1 Introduction**

30 Glacier mass balance observations are important for studies of climate change, water resources
31 and sea level rise (e.g. IPCC, 2013). Mass balance is the change in mass of a glacier over a
32 stated span of time (Cogley et al., 2011). The mass balance is the sum of surface, internal and
33 basal mass balance components. In situ observations of glacier surface mass balance is termed
34 the *glaciological method* (the terms direct, traditional or conventional method are also used in
35 the literature) where mass balance is measured at point locations, and data are interpolated over
36 the entire glacier surface to obtain glacier-wide averages. Surface mass balance is the sum of
37 surface accumulation and surface ablation and includes loss due to calving. Mass balance can
38 also be assessed indirectly by the *geodetic method* (also called cartographic) where the
39 cumulative mass balance for a period is calculated by differencing digital terrain models
40 (DTMs) and converting the volume change to mass using a density conversion. Whereas the
41 glaciological method measures the surface mass balance, the geodetic method measures the
42 sum of surface, internal and basal mass balances. For a direct comparison of glaciological and
43 geodetic balances methodological differences, such as differences in survey dates (account for
44 ablation or accumulation between the survey dates) and surveyed areas (using the same area
45 and ice divides in both methods) must be considered. In addition, effects of changes in density
46 profiles between the geodetic surveys must be accounted for. Moreover, recent studies have
47 shown that internal and basal melt may be substantial for temperate glaciers, in particular for
48 maritime high-precipitation glaciers that span wide elevation ranges (Alexander et al., 2011;
49 Alexander et al., 2013; Oerlemans, 2013).

50 Comparison of glaciological and geodetic data have revealed both discrepancies and
51 agreements (Cogley, 2009). Several studies on homogenization of mass balance records and
52 uncertainty have been carried out recently (e.g. Thibert et al., 2008; Fischer, 2010; Zemp et al.,
53 2010; Nuth and Kääb, 2011; Huss et al., 2015). A joint paper from the workshop on
54 “Measurement and Uncertainty Assessment of Glacier Mass Balance” at the Tarfala Research
55 Station in northern Sweden in 2012 describes a standard procedure for reanalysing mass balance
56 series (Zemp et al., 2013), based on best practices. The reanalysis procedures includes
57 homogenization of glaciological and geodetic balances, assessment of uncertainty, validation,
58 and calibration, if necessary. It recommended that mass balance series longer than 20 years
59 should always be reanalysed.

60 Homogenization of mass balance series can be defined as the procedure to correct artefacts and
61 biases that are not natural variations of the signal itself, but originate from changes in
62 instrumentation or changes in observational or analytical practice (Cogley et al., 2011). In the
63 glaciological method, common inhomogeneities are change in method (e.g. from contour line
64 to altitude-profile method), change in observational network, use of different glacier basins and
65 changes in area and elevation over time. In the geodetic method, inhomogeneity may stem from
66 surveys using different sources and methods (e.g from analogue contour lines to digital point
67 clouds), geo-referencing and projection of the data set, and software. When calculating the
68 geodetic balance it is important that independent data or stable terrain outside the glaciers are
69 used to check the individual DTMs. DTMs should be co-registered (Kääb, 2005) or even
70 reprocessed from original survey data if needed (Koblet et al., 2010). Uncertainty is not only
71 dependent on the standard error of the individual elevation differences, but is also dependent
72 on the size of the averaging area and the scale of the spatial correlation (Rolstad et al., 2009;
73 Magnússon et al., 2016).

74 In Norway, the contribution of glacier melting to runoff instigated systematic mass balance
75 studies on several glaciers in the 1960s. Mass balance programmes have been conducted on
76 more than 40 glaciers for shorter or longer periods (Andreassen et al., 2005; Kjølmoen et al.,
77 2011).

78 In this paper, we compare homogenised glaciological and geodetic mass balance for the 10
79 Norwegian glaciers with long-term mass balance series, whereof nine of them are considered
80 key climate change reference series in Norway (Fleig et al., 2013) and seven of them are used
81 as reference glaciers for the World Glacier Monitoring Service (WGMS, 2013). The data are
82 widely used, for modelling and statistical analyses and at different scales from local studies to
83 global estimates (e.g. Rasmussen, 2004; Nesje and Matthews, 2012; Engelhardt et al., 2013;
84 Trachsel and Nesje, 2015; Zemp et al., 2015; Treichler and Kääb, 2016).

85 The reanalysis of the mass balance series included (i) homogenisation of both glaciological and
86 geodetic observation series, (ii) uncertainty assessment, (iii) estimates of generic differences
87 including estimates of internal and basal melt, (iv) validation, and, if needed, (v) partly
88 calibration of mass balance series.

89 A large set of metadata, observations, calculations and procedures were analysed: 454 years of
90 glaciological mass balance data, 34 geodetic surveys/maps and 21 periods of concurrent data.
91 The analysed glaciers covered an area of 134 km² ranging from 60.5 to 70.1 degrees North.

93 **2 Study glaciers**

94 The ten glaciers selected for this study all have long-term mass-balance programmes and
95 geodetic surveys that cover (the larger part of) the period with annual measurements (Table 1,
96 Fig. 1). Glaciers with short-term series without concurrent geodetic surveys are not considered
97 here. The glaciological series are continuous, except Langfjordjøkelen where glaciological
98 measurements are lacking for two years (1994, 1995). The longest series is Storbreen where
99 measurements began already in 1949; the shortest series are for Hansebreen, Austdalsbreen and
100 Langfjordjøkelen where measurements began in the late 1980s (Table 1). All glaciers are part
101 of a glacier complex (thus, sharing border with at least one other glacier flow unit), except for
102 Storbreen (Andreassen et al., 2012b). The glaciers in southern Norway are located along a west-
103 east transect, extending from a wet maritime climate, where Ålfotbreen and Hansebreen are
104 located, to drier conditions in the interior, where Gråsubreen is located (Fig. 1). Engabreen and
105 Langfjordjøkelen are located near the coast in the central and northern parts of Norway,
106 respectively, and represent the glaciers with the lowest minimum and maximum elevation,
107 respectively. The glaciers range greatly in size from 2.2 km² (Gråsubreen) to 46.6 km²
108 (Nigardsbreen). One glacier, Austdalsbreen, calves into a regulated lake.

109 Norwegian glaciers have retreated throughout the twentieth century, although several periods
110 of advance have also occurred. The most recent advance started in the late 1980s on many
111 maritime glaciers, but culminated around 2000 (Andreassen et al., 2012b). Mass balance results
112 show different behaviours of the ten study glaciers. The northernmost glacier,
113 Langfjordjøkelen, and the three interior (easternmost) glaciers in southern Norway (Storbreen,
114 Hellstugubreen and Gråsubreen) have steadily lost mass during the past 50 years, greatest in
115 Langfjordjøkelen (Andreassen et al., 2012a). The other six glaciers are maritime ice cap outlets,
116 that had a mass surplus, mainly due to higher snow accumulation in the 1990s, although all
117 have lost mass since 2000 (Andreassen et al., 2005; 2012b; Kjølmoen et al., 2011). There is
118 significant variability in mass turnover between the study glaciers, from annual
119 accumulation/ablation of about 1-2 m w.e. for the interior glaciers to 3-6 m w.e. for the maritime
120 glaciers on the west coast (Andreassen et al., 2005).

122 **3 Data and methods**

123 In this chapter, we describe the data and methods used for calculating glaciological and geodetic
124 mass balance and for the reanalysis undertaken. We describe the original data sets, the
125 homogenization of these and provide uncertainty assessments of systematic and random errors.

126 **3.1 Glaciological mass balance**

127 **3.1.1 Surface mass balance observations**

128 NVE's surface mass-balance series contain annual (net), winter and summer balances. Details
129 on the observation programme including maps of the annual monitoring network are found in
130 NVE's report series Glaciological investigations in Norway (e.g., Kjølmoen and others, 2011,
131 all reports are available at <http://www.nve.no/glacier>). Methods used to measure mass balance
132 in the field have in principle remained unchanged over the years, although the number of
133 measurements has varied (Andreassen et al., 2005). The winter balance is measured in spring
134 by probing to the previous year's summer surface along regular profiles or grids, typical values
135 being 50-150 probings on each glacier every year (Fig. 2). Snow density is measured in pits and
136 with coring at one or two locations at different elevations on each glacier. Stake readings and
137 snowdepth corings are used to verify the probings. Summer and annual balances are obtained
138 from stake measurements using density estimates of remaining snow (usually 600 kg/m^3),
139 melted firn ($650\text{-}800 \text{ kg/m}^3$) and ice (900 kg/m^3) (e.g. Kjølmoen et al., 2011). The number of
140 stake positions varies from glacier to glacier and through time, typical values being 5–15. Stake
141 density is highest on the smallest glacier, $6/\text{km}^2$ on Gråsubreen, and lowest on the largest
142 glaciers, $0.2/\text{km}^2$ on Nigardsbreen and Engabreen. The annual calving from Austdalsbreen is
143 calculated from measured ice velocity near the terminus, surveyed autumn terminus positions
144 and estimated mean ice thickness (Elvehøy, 2011), following Funk and Rötlişberger (1989).

145 To calculate glacier-wide winter (B_w), summer (B_s) and annual (B_a) balances, the point
146 measurements are interpolated to area-averaged values. In the first years this was done by the
147 contour line method, while since the mid/end of the 1980s this has been done using the profile
148 method. The shift in method was mainly a consequence of a reduction in the observing network
149 on many of the maritime glaciers. Furthermore, investigations had showed that annual balance
150 measured at stakes correlated well with glacier-wide annual balance and that the fieldwork
151 could be simplified (Roald, 1973). In the contour line method, the point measurements were
152 plotted on a map and isolines of mass balance were drawn for both winter and summer balances

153 (Fig. S1). The areas between adjacent isolines within each altitudinal interval (50 or 100 m)
154 were integrated using a planimeter, and the total amount of accumulation and ablation was
155 calculated for each altitude interval. In the profile method, the point measurements versus
156 altitude are plotted and interpolated balance profiles are drawn to obtain mass balance values
157 for each altitudinal interval (Fig. 3). The elevation of point measurements and area distribution
158 are taken from the most recent map/digital terrain model of the glacier. When a new map has
159 been constructed, it was used for the calculations from then and onwards. However, there may
160 be considerable time lag (up to 30 years) between the mass balance year and the reference area
161 used for calculating mass balance.

162 Glaciological balances are reported as conventional surface balances, i.e. internal and basal
163 balances have not been part of the observational programme and are not accounted for in the
164 published mass balance records.

165 3.1.2 Homogenization of surface mass balance

166 Homogenizing a surface mass balance series may involve different steps and will differ from
167 glacier to glacier according to the richness of the data material as well as the time available for
168 the analysis. A thorough homogenizing process was applied to four of the glaciers
169 (Nigardsbreen, Engabreen, Ålfotbreen and Hansebreen), as the first comparison of geodetic and
170 glaciological balances indicated rather large discrepancies between the methods (Elvehøy et al.,
171 2016; Kjöllmoen, 2016a; 2016b). This detailed homogenisation process included going through
172 the data material for each year to search for inhomogeneities and possible biases in the data
173 calculations. The process included digitisation of point measurements, recalculating the mass
174 balance using homogenized drainage divides, density conversion, and recalculating from
175 contour to profile method for the earlier years. For the other six glaciers, a less detailed
176 procedure was followed, typically including homogenization of the drainage divide and area–
177 altitude distributions. For Austdalsbreen the calculation procedure of losses due to calving was
178 also homogenized.

179 In the following section, we describe in more detail the homogenization of the area–altitude
180 distribution, the change from the contour map method to the profile method, and the calving of
181 Austdalsbreen.

182 **Area–altitude distribution**

183 The annual mass-balance calculations were based on a series of maps for each glacier. When a
184 new map or DTM became available some time after the survey, the mass-balance was
185 calculated from then on using the new map for the stake and sounding elevations and the area–
186 altitude distribution. The changing glacier area and elevation over time is an inhomogeneity
187 common to all mass balance calculation s (Holmlund et al., 2005; Zemp et al., 2013). To
188 minimize the effects of the changing elevation distribution on the results, we recalculated
189 glacier wide balance values for the period of record using both area–altitude distributions. Two
190 approaches were tested, (1) shift: simply using the older map for first half of the period and
191 then using the newer map for the second half, or (2) linear weighting: calculating B_a for all
192 years in the period using both area–altitude distributions and linearly time-averaging between
193 them.

194 The advantage of approach (2) is that the values are interpolated through time, and
195 inhomogeneity is smoothed out. However, for several of the glaciers there is not a linear trend
196 in glacier change. Langfjordjøkelen is the glacier with the strongest thinning and retreat of the
197 10 study glaciers (Andreassen et al., 2012a), and is expected to have the largest sensitivity to
198 the DTM used for the mass balance results. A comparison between the two methods for
199 Langfjordjøkelen and Storbreen shows that the difference between method 1 and 2 is small for
200 the cumulative B_a for both glaciers, -0.18 m w.e. for Langfjordjøkelen for the period 1995-2008
201 and 0.01 m w.e. for Storbreen for the period 1998-2009 (Table 3). Results further reveal that
202 the difference in B_a values for individual years varied between 0.09 and -0.06 m w.e for
203 Langfjordjøkelen and between 0.01 and -0.02 m w.e. for Storbreen. For simplicity, approach
204 (1) was used for the final calculations for all glaciers. For glaciers with strong non-linear
205 changes, normalized front variation series might be used to weight the inter-annual area changes
206 (Zemp et al., 2013), but this was not used in this study.

207 **Contour map to profile method**

208 In the 1980s, a simplification of the observation programme was carried out after statistical
209 analysis of the previous years' accumulation and ablation patterns, especially at large outlet
210 glaciers like Nigardsbreen and Engabreen (Andreassen et al., 2005). The interpolation method
211 was also shifted from the contour to the profile method at the end of the 1980s. However, the
212 profile method can be sensitive to the altitudinal coverage and the spatial pattern of observations
213 (Escher-Vetter, 2009). The profile method relies on the consistency of the annual mass balance
214 gradient. Analyses of the mass balance gradients show vertical profiles of annual and seasonal

215 mass balance are remarkably linear and vary little from year to year (Rasmussen, 2004;
216 Rasmussen and Andreassen, 2005). Studies of Lemon Creek and Taku Glacier, Alaska, show
217 also a consistency of the annual balance gradient (Pelto et al., 2013). Usually the profile method
218 has been used by drawing the area–altitude mass balance curves manually for our mass balance
219 data. To test the sensitivity of the manual drawing on the mass balance results, two of the
220 authors used the point data for Engabreen to draw curves for seven years, 2002-2008. In this
221 period, the glacier had only one stake at the tongue at ~300 m a.s.l. and then about 6 stakes on
222 the ice plateau from ~950 to 1350 m a.s.l. The profile curves were then compared with the
223 curves drawn manually by the principal investigator and there were only minor differences
224 between the drawn curves. The resulting annual B_w , B_s and B_a values calculated from the
225 profiles were in good agreements and were typically within ± 0.1 m w.e. a^{-1} of each other with
226 no outliers. Thus, this test revealed little sensitivity to the subjective judgement in the manual
227 drawing of the annual curves in the profile method. More automated procedures were tested,
228 but were not found suitable due to the data material available.

229 **Calving**

230 For Austdalsbreen, a map from 1966 was originally used for 1988-2008 and the map from 2009
231 since 2009. In the homogenization, mass balance was recalculated using the 2009 ice divide for
232 all years, the 1988 glacier outline and area–altitude distribution for 1988-1998, and the 2009
233 outline and area–altitude distribution from 1999. Due to construction of a hydropower reservoir
234 in front of Austdalsbreen in 1988-89, the lake level was changed from a fixed level around 1156
235 m a.s.l. to a varying level between 1150 and 1200 m a.s.l. The lowest part of the glacier calved
236 off during the first two years. Thus, in the homogenization this was accounted for by removing
237 the calved off part below 1200 m a.s.l. (0.093 km²) from the area–altitude distribution from
238 1990. As part of the homogenization, the annual calving volumes were also recalculated.

239 **3.1.3 Example: homogenization of the Nigardsbreen surface mass balance** 240 **record**

241 Annual glaciological mass balance measurements began on Nigardsbreen in 1962 (Østrem and
242 Karlén, 1962). NVE has carried out the measurements in all years, but many people have been
243 involved in the fieldwork during this period, and several principal investigators have been
244 responsible for the calculations. The original published results show positive mass balance from
245 1962 to 1988 (4.5 m w.e.), a large surplus from 1989 to 2000 (12.9 m w.e.) and near balance (a

246 small deficit) from 2001 to 2013 (-0.96 m w.e.). Detailed glacier maps have been constructed
247 from aerial photographs taken in 1964, 1966/1974 (combined) and 1984, and by laser scanning
248 in 2009 and 2013. The original glaciological mass balance series were compared with geodetic
249 mass balances for the periods 1964-1984, 1984-2013, and revealed large discrepancies. Due to
250 uncertainties of the original map from the 1964 photos constructed in 1965, a new digital point
251 cloud was constructed from the 1964 photos in 2014. The combined 1966/1974 map was made
252 using photos from the two years, and due to the large time gap between the photos and
253 uncertainties in which parts mapped by which photos, the map was not used for the geodetic
254 calculations.

255 All point measurements of snow depths and stakes were identified in data reports and maps,
256 and given positions and altitudes from the relevant DTM. The re-calculation was based on the
257 profile method within the hydrological basin and with the current DTM and ice divide from
258 2009/2013. The review of the historic data sets and the re-calculation process also revealed
259 some errors in the original mass balance calculations in some years, e.g. the handling of summer
260 snow fall and density conversions. These errors were corrected in the re-calculations.

261 The glaciological mass balance methodology has changed through the period of measurements.
262 Five types of inhomogeneities were identified and accounted for in the homogenisation process
263 (Table S1).

264 **Contour line method**

265 From 1962 to 1988, both winter and summer balances were calculated using the contour line
266 method. From 1989, the altitudinal mass balance curves were constructed by plotting point
267 measurements versus altitude. Accordingly, the homogenization involved re-calculation of the
268 period 1962-1988 using the profile method. The curves were manually drawn between the point
269 measurements.

270 **Area–altitude distribution**

271 The original mass balance calculations were based on area–altitude distribution from five maps
272 (1964, 1974, 1984, 2009 and 2013). There were considerable time lags between the mass
273 balance data and the map used for the calculations. Over the years from 1964 to 2013,
274 Nigardsbreen had periods of both shrinking and growing. Hence, the step approach was used
275 where the period between two mappings were divided in two, and each map was applied to half
276 of the period before the mapping year and half of the period after the mapping year.
277 Accordingly, the homogenization involved re-calculation of the periods 1969-73, 1979-87 and

278 1997-2012. This resulted in small changes of the annual B_w , B_s and B_a values, keeping the DTM
279 for the start year for the whole period instead of the step approach would have resulted in a
280 more positive cumulative balance for the first period 1964-1974 (+0.42 m w.e.), nearly no
281 change for 1975-1984 (+0.05 m w.e.), more negative for 1985-2009 (-0.18 m w.e.), and nearly
282 no change for 2010-2013 (+0.05 m w.e.). The overall change in balance after homogenizing the
283 area–altitude distribution was small (0.31 m w.e) for Nigardsbreen, and has thus little impact
284 on the cumulative mass balance.

285 **Snow density conversion**

286 Winter balance calculations are based on measurements of snow depths and snow density. The
287 converting procedure from snow depth to water equivalent has varied through the years. For
288 the first four decades (from 1960s to 1990s) a precise documentation of the converting
289 procedure is lacking. However, for some of the years, it appears that an average density (ρ_{av}) of
290 the snow pack was used for each snow depth (c_a) expressed as: $b_w = c_a \text{ (m)} * \rho_{av} \text{ (kg m}^{-3}\text{)}/1000$.
291 For some other years, a unique snow density for each snow depth was estimated based on the
292 measured density profile. From 2001 and onwards a snow density function derived from the
293 snow density measurements was used to convert snow depths to snow water equivalents.
294 Usually a third degree (or second) polynomial was used, expressed as: $b_w = a * c_a^3 + b * c_a^2 +$
295 $c * c_a + d$ (a, b, c and d are coefficients). In the homogenization process a density function was
296 used for 40 of the 52 years. For twelve of the years, the original water equivalent values (b_w)
297 were kept due to lacking data or difficulties in data interpretation.

298 **Ice divide**

299 The ice divide used in the calculations was made for each map, and thus varied between the
300 mappings. The DTM derived from the laser scanning is considered much more accurate than
301 the DTM derived from the aerial photos used for the older maps, in particular in the flat
302 accumulation area where the ice divide of the glacier is located. Although the ice divide may
303 have moved through time, it is not possible to determine this with the map material available.
304 Thus, assuming that the ice divide had been unchanged over the period of record, the divide
305 constructed from the laserscanned DTMs from 2009 and 2013 were considered the most
306 accurate (a comparison of 2009 and 2013 divides showed similar divides, a combination of
307 them was used to obtain full spatial coverage). Accordingly, the homogenization involved re-
308 calculation of the period 1962-2012, using the ice divide from 2009/2013.

309 **Glacier boundaries**

310 From 1962 to 1967, the mass balance for Nigardsbreen was calculated using the glaciological
311 basin, i.e. the area draining ice to the glacier terminus, thus excluding the southeastern and
312 northeastern fringes that do not flow into the main glacier (Fig. 4). The hydrological basin, i.e.
313 the surface area draining water to the lake, Nigardsbrevatn, has been used for the glaciological
314 mass balance calculations since 1968. The influence on the volume change calculations of the
315 different drainage basins was checked for the period 1962-1967 and the area–altitude
316 distribution from DTM1964 using both the hydrological basin (48.3 km²) and the glaciological
317 basin (40.9 km²). The test revealed almost identical results for the average annual balance, but
318 with small interannual variations. The hydrological drainage basins based on the surveys from
319 1964, 1984, 2009 and 2013 are quite similar in both area extent and pattern, but not exactly
320 congruent. The ice divide from 2009/2013 was used for all four DTMs. However, different
321 interpretations and veritable changes of the ice margin reveal four drainage basins with some
322 minor differences. The hydrological basin area was 48.3 km² (1964), 48.1 km² (1984), 47.2 km²
323 (2009) and 46.6 km² (2013), respectively. The 1964 basin has the greatest area and the most
324 extended frontal ice margin (Fig. 4).

325 **3.2 Internal mass balance calculation**

326 Internal and basal balances are not measured, but need to be accounted for when comparing
327 glaciological with geodetic balances. Melting occurs within a glacier if the temperature is at
328 melting point and there is a source of energy (Cuffey and Paterson, 2010). Flowing water that
329 is warmer than the ice may cause melting by direct heat transfer or by loss of potential energy,
330 which dissipates as heat (Cuffey and Paterson, 2010). Theoretic calculations has suggested that
331 internal ablation can be a significant term for Nigardsbreen (Oerlemans, 2013) and can
332 contribute as much as 10% to the total ablation of Franz Josef Glacier (Alexander et al., 2011).
333 In this study, we estimated internal and basal ablation due heat of dissipation based on
334 Oerlemans (2013). Ablation due to rain (Alexander et al., 2011) was considered negligible, as
335 most of this melting affects snow, firn and ice at the surface, rather than the subglacial and basal
336 system. Other terms such as geothermal heat and refreezing of melt water below the previous
337 summer' surface were also considered negligible as they were assumed to be insignificant in
338 this climate and will to some degree cancel out.

339 Melt by dissipation of energy, M, was calculated by the formula

$$340 \quad M = \frac{\sum h g P_h A_h (h - b_L)}{A L_m} \quad (1)$$

341 where g is the acceleration of gravity, h is mean elevation of elevation interval used in surface
342 mass balance calculations, P_h is precipitation at h , A_h is glacier area of elevation interval h , b_L
343 is bed elevation at glacier snout, A is total glacier area and L_m is latent heat of fusion. This
344 formula is based on formulas (8) and (9) in Oerlemans (2013), but calculates the effect at each
345 elevation interval used in surface mass balance for the given glacier. Precipitation was
346 calculated as a linear function of elevation. Daily precipitation was extracted from data version
347 1.1.1 at www.senorge.no (Saloranta, 2014). The seNorge (in English ‘see Norway’) dataset
348 provides daily gridded data of temperature, precipitation and snow amounts in Norway from
349 1957 to present using data from all available stations of the Meteorological Institute (e.g.
350 Saloranta, 2012).

351 **3.3 Geodetic mass balance**

352 **3.3.1 Surveys**

353 The geodetic surveys used in this paper were constructed from different sources and methods
354 (Table 2). Before 2001, surveys were based on vertical aerial photos. Most of the surveys from
355 1950s to the 1980s are contour maps constructed from vertical aerial photographs using
356 analogue photogrammetry. These analogue contour maps were digitised at the end of the 1990s.
357 In the 1990s, digital terrain models or digital contour maps were usually constructed directly
358 from the aerial photos. Since the first laser scanning of Engabreen in 2001 (Geist et al., 2005),
359 all surveys of the glaciers used in this study have been made from airborne laser scannings,
360 usually in combination with concurrent air photos. A few maps have been reconstructed
361 (Ålfotbreen and Hansebreen 1968, Nigardsbreen 1964) to improve the surveys.

362 **3.3.2 Mass balance calculations**

363 The differences between repeated DTMs should reveal the change in elevation between the
364 corresponding times of data acquisition, and not change due to misalignments of the DTMs. To
365 check for this, for each glacier, the older DTMs were compared with the most recent laser
366 scanned DTM to check for misalignment and shifts. In the following, we describe the
367 homogenization and calculation procedure. All GIS based data processing of maps and DTMs
368 by NVE was done using ArcGIS software (©ESRI), Python (Python Software Foundation) or
369 Surfer software version 12 (Golden Software, Inc. 2014).

370 The following approach was used to test the quality of the DTMs. The latest laser scanned
371 elevation point clouds were considered the most accurate and used to create a 5 or 10 m
372 reference DTM. For surveys available as digitised contour maps, the contour lines were
373 converted to elevation points at vertices along contour lines. Elevation differences were
374 calculated between the reference DTM and the elevation points. For gridded maps, elevation
375 differences, dH, were calculated by DTM differencing on a cell by cell basis. The vertical
376 elevation differences, dH, were compared outside the glacier in stable terrain.

377 The DTMs and contour maps were first checked for horizontal and vertical shifts by plotting
378 vertical difference of the terrain, dH, outside the glacier border against aspect, and dH/tan α
379 against aspect, where α is the angle of the slope (Kääb, 2005; Nuth and Kääb, 2011). In one
380 case, Engabreen 1968, a systematic horizontal shift of 12 meters was detected and the map was
381 shifted prior to the further analysis.

382 To decide whether a DTM should be shifted in vertical direction, a mean error, ε , was calculated
383 from the standard error, σ , of the elevation differences, dH:

$$384 \quad \varepsilon = z \frac{\sigma}{\sqrt{n}} \quad (2)$$

385 Where n are number of independent samples. For a contour map we used n as the number of
386 contours from which we compared the points, for a map constructed from aerial photographs
387 we used n as the number of photos.

388 Only points with slopes less than 30 degrees were considered. Orthophotos and glacier extents
389 were checked to avoid comparing points that were snow covered in one of the surveys. We
390 chose z as 1.96 for achieving a 95% confidence interval assuming that the data are normally
391 distributed. Furthermore, we only shifted if the $\varepsilon < \overline{dH}$ and $\overline{dH} > 1\text{m}$. This may be considered
392 conservative, but contour points outside a glacier are not necessarily representative for the
393 glacier surface.

394 For the further processing, DTM's were created from the contour maps using digitised vertices
395 along the contour lines together with elevation points from the map to convert contour maps to
396 regular grids of 5 or 10 m cell size aligning to the reference DTM. The interpolation function
397 'Topo to Raster' (ArcGIS) (Hutchinson, 1989; Hutchinson and Dowling, 1991) or Kriging
398 (Surfer) were used to obtain surface grids. Various interpolation functions in ArcGIS and Surfer
399 were tested, but had little influence on the results. In a test, the results for Nigardsbreen 1984-
400 2013 were calculated from the contour map (1984) and laser data (2013) to final DTM

401 difference map with both Kriging in Surfer and Topo to Raster in ArcGIS, and gave near
402 identical resulting elevation difference (within ± 0.1 m).

403 Surface elevation changes were calculated for all glaciers and periods by subtracting the DTMs
404 on a cell-by-cell basis.

405 To compare the geodetic mass balance with the glaciological balance, the volume change of
406 ice, snow and firn over a period needs to be converted to mass using a density estimate.
407 Observations of firn thickness and density are in general few and only exist for a few point
408 locations in mainland Norway. In May 1987, a 47 m core was drilled at the highest elevation at
409 Nigardsbreen, revealing a firn/ice transition at 30 m depth (Kawamura et al., 1989). The snow
410 depth was about 6 m giving a firn layer of 24 m at this point. The density of the firn varied from
411 550 to 750 kg m⁻³. At the top of Rembedalskåka at 1850 m a.s.l., in the autumn of 1970, several
412 firn cores were drilled 7 to 10 m into firn probably dating back to 1964. The firn density
413 increased from 600 to 700 kg/m³ in these cores (Laumann, 1972). Unfortunately, no repeat
414 profiles are available to determine changes in the density over time.

415 Since few observations of firn thicknesses and densities are available, it is a common approach
416 to assume that the density profile from the surface to the firn–ice transition remained unchanged
417 between the surveys following Sorge’s law (Bader, 1954). Often an ice density of 900 kg m⁻³
418 has been used to convert volume to mass (e.g. Andreassen, 1999; Haug et al., 2009); other
419 studies have used values of 917 kg m⁻³ (Nuth et al., 2010), or 860 \pm 60 kg m⁻³ (Zemp et al.,
420 2010). Huss (2013) showed that a density conversion factor, $f_{\Delta V}$, of 850 \pm 60 kg m⁻³ is
421 appropriate to convert volume change to mass change for a wide range of conditions. However,
422 for short time intervals (≤ 3 yr), periods with limited volume change, or changing mass balance
423 gradients, the conversion factor can vary much more. Following Huss (2013) we estimated the
424 density correction factor, $f_{\Delta V}$, for each period of the 10 glaciers by:

$$425 \quad f_{\Delta V} = \frac{\Delta \rho V}{\Delta V} + \rho \quad (3)$$

426 where ρ is the bulk density of the glacier including ice, snow and firn and $\Delta \rho$ and ΔV is the
427 change in bulk density and volume, respectively, between the two periods. We used observed
428 ice thicknesses and volume changes and estimated firn thicknesses, density and firn area extent
429 based on calculated area-accumulation ratios and best estimate taking into account the annual
430 balances in the periods prior to the surveys. Obtained values varied between 800 and 899; thus
431 within 850 \pm 60, with the exception of one period for Gråsubreen (1984-1997) that had a lower

432 value. Whereas the firm area can be estimated somewhat more precisely due to observed annual
433 balances and estimates of ELA and AAR and air photos, the values of firm densities and firm
434 depths can only be estimated. We therefore decided to use a density conversion factor, $f_{\Delta V}$ of
435 $850 \pm 60 \text{ kg m}^{-3}$.

436 We thus calculated the geodetic mass balance, B_{geod} , by

$$437 \quad B_{\text{geod}} = \frac{\Delta V \cdot f_{\Delta V}}{\bar{A}} \quad (4)$$

438 where \bar{A} is average glacier area of the two surveys assuming a linear change in time. The glacier
439 area derived from the homogenized ice divides based on the latest laser scanning was used as
440 calculation basis.

441 Finally, the geodetic results were corrected to account for ablation and accumulation between
442 the glaciological and the geodetic surveys. The correction was estimated by using stake readings
443 if available, snow information from www.senorge.no, or modelled using a simple mass balance
444 model with input of temperature and precipitation data from nearby meteorological stations
445 (downloaded from www.eklima.no). The latter approach was also used for estimated the two
446 years (1994 and 1995) of lacking data at Langfjordjøkelen.

447 **3.4 Uncertainty assessment**

448 Uncertainties in glaciological and geodetic mass balances may be systematic or random. Our
449 uncertainty assessment followed the approach recommended by Zemp et al. (2013). We aimed
450 at quantifying random errors by analysing existing data and the processes involved, while
451 eliminating systematic errors through the processes of homogenisation.

452 **3.4.1 Glaciological balances**

453 The uncertainties in glaciological balance were quantified from an analysis of these factors:

- 454 1) Uncertainty of *point measurements* ($\sigma_{\text{glac.point}}$) due to uncertainty in
- 455 - probing to the summer surface (probe may penetrate the summer surface layer or
456 stop at layers above the summer surface, recording or reading may be incorrect),
 - 457 - stakes and towers (stakes may fall down or melt out, towers may be anchored to
458 firn/ice masses at lower depths and thus be vertically displaced),
 - 459 - density measurements of snow (measurement or recording errors, errors or
460 unrepresentative depth-density conversion formula), and

- 461 - density of firn (normally not measured, but estimated).
- 462 2) Uncertainty of *spatial integration* ($\sigma_{\text{glac.spatial}}$) considering
- 463 - number of stakes for each (50) 100 m vertical band used for calculating balances,
- 464 - number of probings for each (50) 100 m vertical bands used for calculating balances
- 465 - effect of areas not covered by stakes or probings due to ice falls and crevasses.
- 466 3) Uncertainty of *glacier reference area* ($\sigma_{\text{glac.ref}}$) due to
- 467 - glacier area–altitude changes
- 468 - problems in determining the ice-divide.

469 As most of the factors in the glaciological error budget could not be quantified from
470 independent measurements, an expert opinion approach was taken. The glaciologist in charge
471 of the measurements quantified the error in collaboration with a glaciologist with modest
472 involvement in the measurements.

473 3.4.2 Geodetic balances

474 The uncertainties of geodetic balance were quantified from an analysis of these factors:

- 475 1) Uncertainty due to *Digital Terrain Models* ($\sigma_{\text{geod.DTM}}$) compared to reference DTM
476 (high accuracy laser), ground control points, surveyed points on the ice surface, if
477 available, and type of data acquisition (laser, high quality photo, low quality photo).
- 478 2) Uncertainty due to *density conversion* (σ_{dc}) using the density conversion factor as
479 described in section 3.3.
- 480 3) Uncertainty of *Internal balance* (σ_{int}) was not subject to any detailed uncertainty
481 analysis due to lack of independent data, but as it is only an estimate we assume an
482 uncertainty of $\pm 33\%$.

483

484 3.4.3 Example: Uncertainty of the Nigardsbreen records

485 The uncertainty in the Nigardsbreen glaciological mass balance totalled $\pm 0.33 \text{ m w.e. a}^{-1}$ (no
486 differentiation was possible between the two periods 1964-1984 and 1984-2013). This
487 uncertainty has three components:

- 488 1) point measurement uncertainty was $\pm 0.25 \text{ m w.e. a}^{-1}$ based on $\pm 0.15 \text{ m w.e. a}^{-1}$ from
489 identifying the summer surface, $\pm 0.20 \text{ m w.e. a}^{-1}$ from stakes and towers, $\pm 0.05 \text{ m w.e. a}^{-1}$
490 from snow density and $\pm 0.02 \text{ m w.e. a}^{-1}$ from firn density,

- 491 2) spatial interpolation uncertainty was ± 0.21 m w.e. a^{-1} , based on ± 0.15 m w.e. a^{-1} from
492 vertical range and coverage, ± 0.10 m w.e. a^{-1} from coverage, ± 0.10 m w.e. a^{-1} from lack
493 of coverage in ice falls and crevassed areas, and
494 3) glacier reference area uncertainty was ± 0.06 m w.e. a^{-1} , based on ± 0.04 m w.e. a^{-1} from
495 ice divide and ± 0.05 m w.e. a^{-1} from DTMs.

496 The uncertainty in the geodetic mass balance totalled ± 0.16 m w.e. a^{-1} for 1964-1984 and ± 0.08
497 m w.e. a^{-1} for 1984-2013. For the first period, the uncertainty in DTMs was 0.16 m w.e. a^{-1} and
498 density conversion was 0.08 m w.e. a^{-1} . For the second period, the uncertainty in DTMs was
499 0.08 m w.e. a^{-1} and density conversion was 0.01 mm w.e. a^{-1} . The uncertainty in internal
500 ablation was estimated to 0.06 m w.e. a^{-1} .

501

502 **4 Results**

503 **4.1 Homogenized balances**

504 The detailed homogenisation of the glaciological mass balances resulted in changes in seasonal,
505 annual and cumulative values.

506 For Nigardsbreen, the homogenized mass balance series over the period 1962-2013 showed a
507 positive mass balance of 13.2 m w.e., which is 5.4 m w.e. less than the cumulative balance of
508 the original series for the same period (Fig. 5, Table S1). The cumulative winter balance was
509 reduced by 4.6 m w.e. (84 % of the total decrease), while the change in cumulative summer
510 balance was -0.9 m w.e. (16 %). Generally, the homogenized mass balance series over the
511 period 1962-2013 gave a lower mean winter balance than the original series, while the mean
512 summer balances were both lower and higher than the original values. The mean winter balance
513 decrease was 0.09 m w.e. a^{-1} , and the mean summer balance change was -0.02 m w.e. a^{-1} . The
514 impact of the five major changes in methodology were difficult to quantify individually, as it
515 was a joint process homogenising the year-by-year data and from this recalculating the mass
516 balance. The homogenisation of ice divide, basin, change of method from contour to profile
517 area–altitude distribution gave small differences if isolated for one change only, typically within
518 ± 0.1 m w.e. The greatest contribution to the cumulative mass balance reduction of 5.4 m w.e.
519 for Nigardsbreen was ascribed to the individual errors detected in the revisit of the data and the
520 calculations.

521 For Ålfotbreen, the homogenized mass balance series over the period 1963-2010 showed a
522 positive mass balance of 4.7 m w.e., a reduction of 1.6 m w.e. compared to the original series
523 for the same period. For Hansebreen over the period 1986-2010 the homogenized cumulative
524 B_a was -15.1 m w.e., a 1.4 m w.e. greater deficit than the original series. For Engabreen, the
525 homogenization resulted in a reduction of the cumulative B_a to 1.5 m w.e. For Hellstugubreen
526 and Langfjordjøkelen, the cumulative mass balance was 1.3 and 1.0 m w.e. less
527 negative, respectively; these changes are mainly attributed to the recalculation of the mass
528 balance using the newer DTMs and homogenous ice divides for the two glaciers. At
529 Austdalsbreen, the mean contribution of calving to the annual balance increased from 0.26 to
530 0.30 m w.e.a⁻¹. Thus, calving represents 11% of the summer balance in the period of
531 measurements (1988-2014). The homogenized cumulative B_a for 1988-2009 is more negative
532 (-9.8 m w.e.) than the original values (-6.4 m w.e.). For the other glaciers there were only minor
533 changes in the cumulative B_a resulting from the homogenizations.

534 **4.2 Internal balance**

535 Results of the internal ablation calculations show that the mean contribution over the period
536 1989-2014 varies from glacier to glacier (Fig. 7). The highest values are for Nigardsbreen and
537 Engabreen), -0.16 and -0.15 m w.e. a⁻¹ respectively. This is due to high precipitation combined
538 with a large elevation range. All other glaciers have small internal ablation rates of 0.01-0.06
539 m w.e. a⁻¹, mainly due to small elevation differences or small precipitation volumes. All values
540 were calculated for a common period (1989-2014) to compare the absolute contribution
541 between the glaciers. For Engabreen the period was divided into two, before and after the
542 subglacial water intakes constructed in 1993, when much of the sub-glacial run-off was
543 captured by the hydropower diversion tunnel. As a result, according to the calculations, the
544 annual contribution from internal ablation decreased from 0.15 to 0.08 m w.e. a⁻¹. The
545 contribution of internal and basal melt varies from year to year due to varying meteorological
546 conditions. For example, for Nigardsbreen, the average annual internal balance over 1989-2013
547 was calculated to be -0.16 ± 0.04 m w.e. a⁻¹. Values for individual years over the period 1962-
548 2014 ranged from -0.09 to -0.24 m w.e. a⁻¹. The mean homogenized surface summer balance
549 was -2.05 m w.e. over the period 1962-2014, so this contribution represents an 8 ± 3 %
550 additional melt from what is measured at the surface. Internal ablation is a significant
551 contribution for the long-term series of Nigardsbreen, amounting to -8.5 ± 2.1 m w.e. for the
552 53 years of measurements over 1962-2014.

553 4.3 Uncertainty and comparison

554 The results from the uncertainty analysis (Table 4) show that largest uncertainties were
555 associated with point measurements on maritime glaciers (above 0.20-0.25 m w.e. a⁻¹), followed
556 by spatial integration at glaciers with few stakes per elevation band (about 0.15-0.21 m w.e. a⁻¹).
557 The largest point errors were on glaciers with a large mass turnover and with challenging
558 probing conditions due to deep snow packs and more uncertain summer surfaces, in particular
559 in years with much snow remaining from the previous year, and difficulties in maintaining the
560 stake network, both in summer and winter season. The largest spatial interpolation errors were
561 typically at the outlet glaciers with a large accumulation plateau draining ice down through a
562 heavily crevassed icefall leading to the snout – making it difficult to measure at all elevations
563 and parts of the glacier. At Nigardsbreen, Engabreen and Rembesdalskåka only 1–2 stakes are
564 available below the main plateau (see Fig. 3 for Nigardsbreen), However, this part cover less
565 than 10 % of the total area, see also Kjöllmoen (2015a) and Elvehøy (2015) for further details.
566 Other glaciers and error components were small, in the range 0.01–0.12 m w.e. a⁻¹.
567 Uncertainties in geodetic mass balances were largest where old maps were used (up to 0.23 m
568 w.e. a⁻¹), but most were in the range 0.05–0.10 m w.e. a⁻¹. The error in density corrections was
569 small (0.05 m w.e. a⁻¹). The uncertainty in internal balance was assumed to be one third of the
570 balance: above 0.06 m w.e. a⁻¹ for three maritime glaciers and very small for the others.

571 Glaciological and geodetic balances were compared for 21 periods (Table 4, Fig. 8). In this
572 comparison, the internal balance was taken into account by subtracting it from the geodetic
573 balance. The discrepancies and tests of the hypothesis are shown in Table 5. Good agreement
574 (less than 0.20 m w.e. a⁻¹) was found for 12 periods, whilst 5 periods showed discrepancies
575 above 0.40 m w.e. a⁻¹. The four remaining periods had discrepancies between 0.26 and 0.32 m
576 w.e. a⁻¹. The data from the maritime glaciers (Engabreen, Nigardsbreen, Ålfotbreen,
577 Hansebreen) deviated the most, in addition to one period for Rembesdalskåka and Storbreen.
578 The glaciological mass balance was more positive than the geodetic for most large deviations,
579 except for the first period of Hansebreen.

580 Uncertainty was included in the comparison in order to test the null hypothesis (H0: “the
581 cumulative glaciological balance is not statistically different from the geodetic balance”) and
582 to check if unexplained discrepancies suggest calibration to be applied (Zemp et al., 2013).
583 Testing at the 95 % acceptance level showed that the null hypothesis was rejected for seven
584 periods: Ålfotbreen (1997-2010), Hansebreen (1988-1997 and 1997-2010), Nigardsbreen

585 (1984-2013) and Engabreen (1969-2001, 2001-2008). Another two periods, Nigardsbreen
586 (1964-1984) and Storbreen (1984-1997), gave deviations above $0.2 \text{ m w.e. a}^{-1}$, but due to the
587 degree of uncertainty, H_0 was not rejected. For the 12 other periods, deviations were smaller
588 than $0.20 \text{ m w.e. a}^{-1}$ and within the uncertainties at the 95 % acceptance level.

589 **4.4 Calibration**

590 Correcting the glaciological mass balance series with geodetic observations is recommended
591 where large, relative to the uncertainties, deviations are detected between glaciological and
592 geodetic balances (Zemp et al., 2013). The deviations found between glaciological and geodetic
593 surveys for several glaciers in our study calls for a calibration for seven of the 21 periods.
594 Previous studies have suggested using statistical variance analysis (Thibert and Vincent, 2009),
595 distributed mass balance modelling (Huss et al., 2009), or by distributing equally the mean
596 annual difference between the homogenized glaciological and geodetic balance (Zemp et al.,
597 2013). In the latter case, the difference in the annual balance B_a is suggested to be fully assigned
598 to the summer balance B_s (Zemp et al., 2013). To calibrate our data series, we used a slightly
599 different approach. The annual correction is the annual difference between the homogenized
600 geodetic and glaciological mass balance, Δ , for each period (Table 5). This annual correction
601 factor was applied to the summer and winter balances according to their relative size. In other
602 words, if summer and winter balances were equal, 50 % of the correction was applied to the
603 summer balance and 50 % to the winter balance. If the absolute summer balance was twice the
604 winter balance, $2/3$ of the correction was applied to the summer balance and $1/3$ to the winter
605 balance. The reasoning behind this was that the size of the error was probably related to the size
606 of the balance. In years with a thick snow layer, the probing to the summer surface and
607 maintenance of the stake network was more uncertain. In years with large melt, maintenance of
608 stake networks was more difficult and the results less accurate.

609 **4.5 Reanalysed glaciological series**

610 The reanalysed glaciological series, resulting from homogenization and calibration, reduced the
611 positive cumulative balances measured at some of the Norwegian glaciers. The major changes
612 in cumulative balances up to and including year 2013 are (the part of reduction due to
613 calibration in parenthesis):

614 1) Engabreen reduced by 20.5 (19.5) m w.e. since 1970

- 615 2) Nigardsbreen reduced by 14.8 (9.4) m w.e. since 1962
- 616 3) Ålfotbreen reduced by 7.5 (5.9) m w.e since 1963
- 617 4) Rembesdalskåka reduced by 5.9 (6.8) m w.e. since 1963
- 618 5) Austdalsbreen reduced by 3.6 m w.e. since 1988

619 For Rembesdalskåka the homogenization resulted in more positive balance; thus the calibrated
620 part is larger than the total reduction. Austdalsbreen was not calibrated, the reduction is only
621 due to the homogenization. The other glaciers had small or no change (within ± 1.3 m w.e.). The
622 reanalysed series show a much more consistent signal than the original data (Fig. 8.). The
623 previously reported difference of the cumulative balances of the maritime and continental
624 glaciers is still present, but much less pronounced. Six glaciers have a large mass loss
625 (cumulative balance between -14 and -22 m w.e.) and four glaciers are nearly in balance
626 (cumulative balance within ± 4 m w.e.). Original data showed a marked surplus for three
627 glaciers (up to 21 m w.e.). A period of surplus is still visible in the data, but now mainly as a
628 transient surplus for the period 1989-1995. The cumulative results further highlight the marked
629 loss of mass during the period after 2000 for all glaciers.

630

631 **5 Discussion**

632 **5.1 Calibration**

633 The resulting cumulative curves after the homogenization and calibration showed that the
634 distinctly positive cumulative mass balances measured at Engabreen and Nigardsbreen were
635 much reduced. When calibrating we accounted for the internal balance by subtracting it from
636 the geodetic mass balance before comparing it with the glaciological. This was done to ensure
637 that the glaciological balance was still the surface mass balance, which is what we measure for
638 all glaciers. The degree of calibration thus also depends on how much internal melt we estimate.
639 The internal ablation rates calculated for the two maritime glaciers, Engabreen and
640 Nigardsbreen, with a large elevation range was significant and represented a marked difference
641 between the glaciological and geodetic methods. For the 49 years compared for Nigardsbreen,
642 internal ablation amounted to nearly -8 m w.e. according to our calculations. Oerlemans (2013)
643 estimated an even higher dissipative melt of -0.23 m w.e. a^{-1} for Nigardsbreen. Using this value
644 would give more than -11 m w.e. resulting from the internal balance over the 49 years. Although
645 both values must be considered only an estimate, it demonstrates how sensitive cumulative

646 series are both to systematic biases and to generic differences between the methods. For
647 Engabreen, almost all the change in cumulative values is due to the calibration of the two
648 geodetic periods and the amount of internal ablation controls the amount of calibration. A
649 higher estimate of internal ablation for this glacier would lead to a smaller difference between
650 the methods and thus less reduction in the mass surplus of the glaciological series. Thus, due
651 care must be shown when interpreting cumulative curves, in particular for glaciers located in
652 high-precipitation regions spanning a large elevation range, such as Engabreen and
653 Nigardsbreen.

654 **5.2 Implications and outlook**

655 The reanalysis processes has altered seasonal, annual and cumulative as well as ELA and AAR
656 values for many of the years for the 10 glaciers presented here. For most glaciers the
657 discrepancy between the ‘original’ glaciological series as published in the series “Glaciological
658 investigations in Norway” (e.g. Kjøllmoen et al., 2011) are small, but for others results differed
659 significantly. We plan to keep the series ‘original’, ‘homogenized’ and ‘calibrated’ in the NVE
660 databases and flag them accordingly as proposed by Zemp et al. (2013), and as exemplified for
661 Nigardsbreen (Table S1). The new reanalysed and thus ‘official’ values will also be made
662 available for download from NVE’s website www.nve.no/glacier. and submitted to WGMS
663 with a remark on the reanalysis status.

664 The level of analysis in the homogenizing process varied between the 10 study glaciers,
665 according to the volume and quality of detailed data and metadata. For some of the glaciers
666 (Nigardsbreen, Engabreen, Ålfotbreen and Hansebreen) a detailed homogenisation process was
667 carried out, going through the data material for each year to search for inhomogenities and
668 possible biases in the data calculations. This should also be considered applied to the other six
669 glaciers, as well as on other glaciers not included here that have shorter series. However, for
670 some glaciers, e.g. Rembesdalskåka and Storbreen, the point data and metadata used for the
671 calculations are simply not available for many of the early years, and a detailed scrutinising of
672 the data and recalculation is not possible.

673 The glaciers that show good agreement between glaciological and geodetic measurements
674 (Austdalsbreen, Storbreen, Hellstugubreen, Gråsubreen, Langfjordjøkelen) have several things
675 in common. Their size is small to medium (2.2-10.6 km²), and they have a higher stake density
676 (1/km²-6/km²) than Nigardsbreen and Engabreen (0.2 km²). Furthermore, most parts are

677 accessible, providing a better stake coverage with altitude. Their altitudinal range is lower and
678 their area-altitude distribution is uniform and not dominated by a flat upper part as in
679 Nigardsbreen and Engabreen. Their glacier basins are also more defined. Furthermore, except
680 for Austdalsbreen, the glaciers had a considerable mass loss and have more or less been
681 constantly losing mass throughout the observation record. Thus, smaller mountain glaciers
682 with negative cumulative balances seems to be easier to measure correctly than the maritime
683 outlet glaciers.

684 As mentioned, on many of the glaciers a change of the observation programme was made after
685 statistical analysis of the previous years' accumulation and ablation patterns in the 1980s. This
686 was done to reduce the amount of fieldwork and hence reduce costs and personnel resources.
687 Studies have pointed out that there can be a good correlation between one stake and the glacier-
688 wide averages (Roald, 1973; Rasmussen and Andreassen, 2005).

689 Glaciological mass balance programmes, based on a minimal network of long-term ablation
690 and accumulation point measurements, is recommended to increase the observational network
691 once every decade in order to reassess the spatial pattern of mass balance (Zemp et al., 2013).
692 The present results may call for a temporarily increased observational network on the glaciers
693 with largest differences between the methods (Engabreen, Nigardsbreen, Ålfotbreen,
694 Hansebreen and Rembesdalskåka) to adjust the observational programmes in order to reduce
695 uncertainty. It should be emphasized that it is far more challenging and expensive to maintain
696 a stake network on a large glacier with high mass turnover like Nigardsbreen, where parts of
697 the glacier must be visited by helicopter and stakes need maintenance several times a year, than
698 the small Gråsubreen where stakes may survive many years and all parts are accessible by foot.
699 However, although smaller glaciers seems to be easier to measure correctly, the maritime outlet
700 glaciers represent by far the largest glacier area and ice volume (Andreassen et al., 2012; 2015).
701 Continued geodetic surveys every 10 years are needed to measure the overall changes and
702 provide data for new reanalysis. The recent geodetic surveys by airborne laser scanning
703 conducted over the period 2008-2013 covered not only the 10 mass balance glaciers presented
704 here, but about 1/3 of the glacial area in Norway. The surveys provide an accurate baseline for
705 future repeated mapping and glacier change detection. They will also be used for a regional
706 overview of glacier volume changes from the 1960s to 2010s.

707

708 **6 Conclusions**

709 This study provided homogenised data series of glaciological and geodetic mass balance for the
710 ten glaciers in Norway with long-term observations. In total, 21 periods of data were compared.
711 Uncertainties were quantified for relevant sources of errors, both in the glaciological and
712 geodetic series.

713 Glaciological and geodetic results were in overall agreement for Langfjordjøkelen,
714 Austdalsbreen, Storbreen, Hellstugubreen and Gråsubreen for the periods considered, but
715 differed for Ålfotbreen (1 of 3 periods), Hansebreen (both periods), Engabreen (both periods),
716 Rembesdalskåka (1 of 2 periods) and Nigardsbreen (1 of 2 periods). Whereas the homogenized
717 glaciological surface mass balance for these glaciers shows a clear cumulative mass surplus
718 over the period of records, the geodetic observations show glaciers in near balance or with a
719 deficit. The glaciological method measures the surface mass balance, while the geodetic method
720 measures surface, internal and basal mass balances. The contribution from internal and basal
721 mass balances was calculated and revealed values > 0.1 m w.e. a^{-1} for Nigardsbreen and
722 Engabreen. Internal and basal melting may therefore represent a significant contribution to the
723 mass balance for long-term series, in particular for glaciers in a wet climate with wide elevation
724 range.

725 Although part of the discrepancy between the glaciological and geodetic methods could be
726 explained by homogenization and by the estimated contribution from internal and basal melt,
727 the discrepancy is large for several periods. For 9 of the 21 periods compared the unexplained
728 discrepancy between the methods amounts to >0.20 m w.e. a^{-1} . The reanalysis resulted in a
729 reduction in balances up to 0.58 m w.e. a^{-1} .

730 The reanalysed series shows a more spatially coherent signal over the period of measurements
731 than previously reported: six glaciers have a significant mass loss and four glaciers are nearly
732 in balance. All glaciers have lost mass after year 2000. The reanalysis effort has therefore
733 contributed towards a better understanding of Norwegian glacier mass balance changes since
734 the 1960s.

735

736

737 **Acknowledgements**

738 The authors thank M. Zemp, World Glacier Monitoring Service, for valuable support and
739 discussions during the work with this paper. We thank J. Oerlemans for providing advice on
740 the calculation of internal ablation. We thank Tomas Johannesson, Mauri Pelto, an anonymous
741 referee and the scientific editor Etienne Berthier for valuable comments to our manuscript in
742 The Cryosphere Discussions. John Brittain is thanked for proofreading the paper. We thank
743 Statkraft AS for providing support to the laser-scanning campaigns. The laser scannings were
744 also supported through the project „Mapping the Surface and surface changes of glaciers and
745 ice caps i Norway, Iceland and Greenland with LiDAR“, funded by Nordisk Ministerråd. This
746 publication is contribution number 78 of the Nordic Centre of Excellence SVALL, “Stability
747 and Variations of Arctic Land Ice”, funded by the Nordic Top-level Research Initiative (TRI).

748

749 **References**

- 750 Alexander, D., Davies, T., and Schulmeister, J.: Basal melting beneath a fast-flowing temperate
751 tidewater glacier. *Ann. Glaciol.*, 54(63), doi:10.3189/2013AoG63A259, 2013.
- 752 Alexander, D., Shulmeister, J., and Davies, T.: High basal melting rates within high-
753 precipitation temperate glaciers. *J. Glaciol.*, 57(205), 789-795, 2011.
- 754 Andreassen, L. M.: Comparing traditional mass balance measurements with long-term volume
755 change extracted from topographical maps: a case study of Storbreen glacier in Jotunheimen,
756 Norway, for the period 1940–1997. *Geogr. Ann.*, 81A(4), 467–476, 1999.
- 757 Andreassen, L. M., Elvehøy, H., Kjøllmoen, B., Engeset, R. V., and Haakensen, N.: Glacier
758 mass-balance and length variation in Norway, *Ann. Glaciol.*, 42, 317–325, 2005.
- 759 Andreassen, L.M., Huss, M., Melvold, K., Elvehøy, H., and Winsvold, S. H.: Ice thickness
760 measurements and volume estimates for glaciers in Norway. *Journal of Glaciology*, 61 (228),
761 doi: 10.3189/2015JoG14J161, 2015.
- 762 Andreassen, L. M., Kjøllmoen, B., Rasmussen, A., Melvold, K., and Nordli, Ø.:
763 Langfjordjøkelen, a rapidly shrinking glacier in northern Norway, *J. Glaciol.*, 58, 581–593,
764 2012a.
- 765 Andreassen, L. M., Winsvold, S. H., Paul, F., and Hausberg, J. E.: Inventory of Norwegian
766 Glaciers, NVE Rapport 38, Norwegian Water Resources and Energy Directorate, 2012b.

767 Bader, H.: Sorge's law of densification of snow on high polar glaciers, *J. Glaciol.*, 2, 319–323,
768 1954.

769 Cogley, J. G.: Geodetic and direct mass balance measurements: comparison and joint analysis,
770 *Ann. Glaciol.*, 50, 96–100, 2009.

771 Cogley, J. G., Hock, R., Rasmussen, L. A., Arendt, A. A., Bauder, A., Braithwaite, R. J.,
772 Jansson, P., Kaser, G., Möller, M., Nicholson, L., and Zemp, M.: Glossary of Glacier Mass
773 Balance and Related Terms, IHP-VII Technical Documents in Hydrology No. 86, IACS
774 Contribution No. 2, Paris, UNESCO-IHP, 114 pp., 2011.

775 Cuffey, K. M. and Paterson, W. S. B.: *The Physics of Glaciers*, 4. edn., Butterworth-
776 Heinemann, Oxford, 704 pp., 2010.

777 Elvehøy, H.: Reanalysing of a mass balance record. Engabreen 1970-2014. NVE Rapport X,
778 Norwegian Water Resources and Energy Directorate, 2016.

779 Elvehøy, H.: Austdalsbreen. in Kjøllmoen, B., L.M. Andreassen, H. Elvehøy, M. Jackson and
780 R.H. Giesen.: Glaciological investigations in Norway in 2010. NVE Report 2, 2011.

781 Engelhardt, M., Schuler, T. V., and Andreassen, L.M. Glacier mass balance of Norway 1961–
782 2010 calculated by a temperature-index model. *Annals of Glaciology* 54(63) 2013
783 10.3189/2013AoG63A245.

784 Escher-Vetter, H., Kuhn, M., and Weber, M.: Four decades of winter mass balance of
785 Vernagtferner and Hintereisferner, Austria: methodology and results, *Ann. Glaciol.*, 50, 87–95,
786 2009.

787 Fischer, A.: Glaciers and climate change: Interpretation of 50 years of direct mass balance of
788 Hintereisferner, *Global Planet. Change*, 71, 13–26, 2010.

789 Fleig, A., Andreassen, L.M., Barfod, E., Haga, J., Haugen, L.E., Hisdal, H., Melvold, K., and
790 Saloranta, T: Norwegian Hydrological Reference Dataset for Climate Change Studies. NVE
791 Rapport 2, 2013.

792 Funk, M. and Röthlisberger, H.: Forecasting the effect of a planned reservoir which will
793 partially flood the tongue of Unteraargletcher in Switzerland. *Annals of Glaciology*, 13, 76–81,
794 1989.

795 Geist, T., Elvehøy, H., Jackson, M., and Stötter, J.: Investigations on intra-annual elevation
796 changes using multitemporal airborne laser scanning data: Case study Engabreen, Norway.
797 *Ann. Glaciol.*, 42, 195-201, 2005.

798 Haug, T., Rolstad, C., Elvehøy, H., Jackson, M., and Maalen-Johansen, I.: Geodetic mass
799 balance of the western Svartisen ice cap, Norway, in the periods 1968–1985 and 1985–2002,
800 *Ann. Glaciol.*, 50, 119–125, 2009.

801 Holmlund, P., Jansson, P., and Pettersson, R.: A re-analysis of the 58 year mass balance record
802 of Storglaciären, Sweden, *Ann. Glaciol.*, 42, 389–394, 2005.

803 Huss, M.: Density assumptions for converting geodetic glacier volume change to mass change,
804 *The Cryosphere*, 7, 877-887, doi:10.5194/tc-7-877-2013, 2013.

805 Huss, M., Dhulst, L., and Bauder, A.: New long-term mass-balance series for the Swiss Alps.
806 *J. Glaciol.*, 61(227), 551-562, , doi: 10.3189/2015JoG15j015, 2015.

807 IPCC: Climate Change 2013: The Physical Science Basis. Contribution of Working Group I to
808 the Fifth Assessment Report of the Intergovernmental Panel on Climate Change [Stocker, T.F.,
809 D. Qin, G.-K. Plattner, M. Tignor, S.K. Allen, J. Boschung, A. Nauels, Y. Xia, V. Bex and P.M.
810 Midgley (eds.)]. Cambridge University Press, Cambridge, United Kingdom and New York,
811 NY, USA, 1535 pp, 2013.

812 Kääh, A.: Remote sensing of mountain glaciers and permafrost creep. Geographisches Institut
813 der Universität Zürich, Zürich, 2005.

814 Kawamura, T., Y. Fujii, K. Satow, K. Kamiyama, K. Izumi, T. Kameda, O. Watanabe, S.
815 Kawaguchi, B. Wold and Y. Gjessing. Glaciological characteristics of cores drilled on
816 Jostedalsbreen, Southern Norway. Proceedings on the NIPR Symposium on Polar Meteorology
817 and Glaciology No 2, p 152-160, 1989.

818 Kjöllmoen, B.: Reanalysing a glacier mass balance measurement series – Nigardsbreen 1962-
819 2013. NVE Rapport X, Norwegian Water Resources and Energy Directorate, 2016a.

820 Kjöllmoen, B.: Reanalysing a glacier mass balance measurement series – Ålfotbreen (1963-
821 2010) and Hansebreen (1986-2010). NVE Rapport X, Norwegian Water Resources and Energy
822 Directorate, 2016b.

823 Kjöllmoen, B. (ed.), Andreassen, L. M., Elvehøy, H., Jackson, M., and Giesen, R. H.:
824 Glaciological investigations in Norway in 2010. NVE Report 2, 2011.

825 Koblet T., Gärtner-Roer, I., Zemp, M., Jansson, P., Thee, P., Haeberli, W., and Holmlund, P.:
826 Reanalysis of multi-temporal aerial images of Storglaciären, Sweden (1959–99) – Part 1:
827 Determination of length, area, and volume changes. *Cryosphere*, 4, 333-343, 2010.

828 Laumann, T. Snø, firn og is – en undersøkelse på Hardangerjøkulen. Cand.real thesis, Dept. of
829 Geography, University of Oslo, 40 p + figures, 1972.

830 Magnússon, E., Muñoz-Cobo Belart, J., Pálsson, F., Ágústsson, H., and Crochet, P.: Geodetic
831 mass balance record with rigorous uncertainty estimates deduced from aerial photographs and
832 lidar data – Case study from Drangajökull ice cap, NW Iceland, *The Cryosphere*, 10, 159-177,
833 doi:10.5194/tc-10-159-2016, 2016.

834 Nesje, A. and Matthews, J.A.: The Briksdalsbre Event: A winter precipitation-induced decadal-
835 scale glacial advance in southern Norway in the AD 1990s and its implications. *The Holocene*.
836 DOI: 10.1177/0959683611414938, 2012.

837 Nuth, C. and Kääb, A.: Co-registration and bias corrections of satellite elevation data sets for
838 quantifying glacier thickness change. *The Cryosphere*, 5, 271–290, 2011.

839 Nuth, C., Moholdt, G., Kohler, J., Hagen, J. O., and Kääb, A.: Svalbard glacier elevation
840 changes and contribution to sea level rise. *J. Geophys. Res.*, 115, F01008,
841 doi:10.1029/2008JF001223, 2010.

842 Oerlemans, J.: A note on the water budget of temperate glaciers. *The Cryosphere*, 7, 1557–
843 1564, doi:10.5194/tc-7-1557-2013, 2013.

844 Pelto, M., Kavanaugh, J., and McNeil, C.: Juneau Icefield Mass Balance Program 1946–2011,
845 *Earth Syst. Sci. Data*, 5, 319-330, doi:10.5194/essd-5-319-2013, 2013.

846 Rasmussen, L.A. 2004. Altitude variation of glacier mass balance in Scandinavia. *Geophys.*
847 *Res. Lett.*, 31(13), L13401. (10.1029/2004GL020273.)

848 Rasmussen, L. A. and Andreassen, L.M.: Seasonal mass balance gradients in Norway. *Journal*
849 *of Glaciology*. 51(175), 601-606, 2005.

850 Roald, L.: En undersøkelse over sambandet mellom nettobalansen malt på enkelte staker og
851 breens totale nettobalanse. In Tvede, A. M. (ed.): *Glasiologiske undersøkelser i Norge 1971*.
852 NVE rapport, 2, Norwegian Water Resources and Energy Directorate, 1973.

853 Rolstad, C., Haug, T., and Denby, B.: Spatially integrated geodetic glacier mass balance and its
854 uncertainty based on geostatistical analysis: application to the western Svartisen ice cap,
855 Norway. *J. Glaciol.*, 55, 666–680, 2009.

856 Saloranta, T. M.: Simulating snow maps for Norway: description and statistical evaluation of
857 the seNorge snow model, *The Cryosphere*, 6, 1323–1337, doi:10.5194/tc-6-1323-2012, 2012.

858 Saloranta, T. M.: New version (v.1.1.1) of the seNorge snow model and snow maps for Norway,
859 Rapport 6-2014, Norwegian Water Resources and Energy Directorate, Oslo, Norway, 30 pp.,
860 available at: http://webby.nve.no/publikasjoner/rapport/2014/rapport2014_06.pdf, 2014.

861 Thibert, E., Blanc, R., Vincent, C., and Eckert, N.: Glaciological and volumetric mass balance
862 measurements error analysis over 51 years for the Sarennes glacier, French Alps, *J. Glaciol.*,
863 54, 522–532, 2008.

864 Thibert, E. and Vincent, C.: Best possible estimation of mass balance combining glaciological
865 and geodetic methods, *Ann. Glaciol.*, 50, 112–118, 2009.

866 Trachsel, M. and Nesje, A.: Modelling annual mass balances of eight Scandinavian glaciers
867 using statistical models, *The Cryosphere*, 9, 1401–1414, doi:10.5194/tc-9-1401-2015, 2015.

868 Treichler, D. and Kääh, A.: ICESat laser altimetry over small mountain glaciers, *The*
869 *Cryosphere Discuss.*, doi:10.5194/tc-2015-234, in review, 2016.

870 WGMS: Glacier Mass Balance Bulletin No. 12 (2010–2011). Zemp, M., Nussbaumer, S. U.,
871 Naegeli, K., Gärtner-Roer, I., Paul, F., Hoelzle, M., and Haeberli, W. (eds.),
872 ICSU(WDS)/IUGG(IACS)/UNEP/UNESCO/WMO, World Glacier Monitoring Service,
873 Zurich, Switzerland, 106 pp., publication based on database version: doi:10.5904/wgms-fog-
874 2013-11, 2013.

875 Zemp, M. Frey, H, Gärtner-Roer, I, Nussbaumer, S. U., Hoelzle, M., Paul, F., Haeberli, W.,
876 Denzinger, F., Ahlstrøm, A. P., Anderson, B., Bajracharya, S., Baroni, C., Braun, L. N.,
877 Cáceres, B. E., Casassa, G., Cobos, Guillermo., Dávila, L. R., Delgado Granados, H., Demuth,
878 M. N., Espizua, L., Fischer, A., Fujita, K., Gadek, B., Ghazanfar, A., Hagen, J. O., Holmlund,
879 P., Karimi, N., Li, Zhongqin., Pelto, M., Pitte, P., Popovnin, V. V., Portocarrero, C. A., Prinz,
880 R., Sangewar, C. V., Severskiy, I., Sigurðsson, O., Soruco, A., Usubaliev, R., Vincent, C..
881 Historically unprecedented global glacier decline in the early 21st century. *Journal of*
882 *Glaciology*, 61, 228, doi: 10.3189/2015JoG15J017, 2015.

883 Zemp, M., Jansson, P., Holmlund, P., Gärtner-Roer, I., Koblet, T., Thee, P., and Haeberli, W.:
884 Reanalysis of multi-temporal aerial images of Storglaciären, Sweden (1959–99) – Part 2:
885 Comparison of glaciological and volumetric mass balances, *The Cryosphere*, 4, 345–357,
886 doi:10.5194/tc-4-345-2010, 2010.

887 Zemp, M., Thibert, E., Huss, M., Stumm, D., Rolstad Denby, C., Nuth, C., Nussbaumer, S. U.,
888 Moholdt, G., Mercer, A., Mayer, C., Joerg, P. C., Jansson, P., Hynek, B., Fischer, A., Escher-
889 Vetter, H., Elvehøy, H., and Andreassen, L. M.: Reanalysing glacier mass balance measurement
890 series, *The Cryosphere*, 7, 1227–1245, doi:10.5194/tc-7-1227-2013, 2013.

891 Østrem, G., and Karlen, V.: Nigardsbreens hydrologi 1962. *Norsk Geografisk Tidsskrift*, 18
892 (1962-62), p. 156-202, doi: 10.1080/00291956108551796, 1962.

893

894 **Tables**

895 Table 1. Overview of the 10 glaciers used in this study, their characteristics, and glaciological and
 896 geodetic surveys used in this study. Period is period of mass balance observations, years is number of
 897 mass balance years up to and including 2014. Elevation min and max (m a.s.l.), slope (degree) and
 898 area (km²) refers to the latest survey. NVE-ID is the ID in the latest inventory (Andreassen et al.,
 899 2012b). See Figure 1 for location and Table 2 for details on geodetic surveys. REMB: 1066-1854

900

| No | Name | NVE-ID | Period | Years | Elmin | Elmax | Area | Slope | Geodetic surveys | n |
|-----|------------------|--------|--------|-------|-------|-------|-------|-------|------------------------|----|
| 1 | Ålftobreen | 2079 | 1963- | 52 | 903 | 1382 | 4.5 | 10 | 1968, 1988, 1997, 2010 | 4 |
| 2 | Hansebreen | 2085 | 1986- | 29 | 930 | 1327 | 3.1 | 9 | 1968, 1988, 1997, 2010 | 4 |
| 3 | Nigardsbreen | 2297 | 1962- | 53 | 313 | 1952 | 46.6 | 8 | 1964, 1984, 2009, 2013 | 4 |
| 4 | Austdalsbreen | 2478 | 1988- | 27 | 1200 | 1747 | 10.6 | 6 | 1988, 2009 | 2 |
| 5 | Rembesdalskåka | 2968 | 1963- | 52 | 1066 | 1854 | 17.3 | 4 | 1961, 1995, 2010 | 3 |
| 6 | Storbreen | 2636 | 1949- | 66 | 1400 | 2102 | 5.1 | 14 | 1968, 1984, 1997, 2009 | 4 |
| 7 | Hellstugubreen | 2768 | 1962- | 53 | 1482 | 2229 | 2.9 | 13 | 1968, 1980, 1997, 2009 | 4 |
| 8 | Gråsubreen | 2743 | 1962- | 53 | 1833 | 2283 | 2.1 | 12 | 1984, 1997, 2009 | 3 |
| 9 | Engabreen | 1094 | 1970- | 45 | 89 | 1574 | 36.8 | 7 | 1968, 2001, 2008 | 3 |
| 10 | Langfjordjøkelen | 54 | 1989-* | 24 | 302 | 1050 | 3.2 | 13 | 1966, 1994, 2008 | 3 |
| Sum | | | | 454 | | | 132.2 | | | 34 |

901 **1994 and 1995 were not measured*

902 Table 2. Geodetic surveys of the 10 glaciers used in this study. Method: a=airborne,
 903 P=photogrammetry, L=laser scanning. A/D: A= analogue constructed, later digitised, D=digital
 904 constructed. Res. = Resolution, contour interval on glacier for contours, resolution of DTM where
 905 regular grids were constructed, points/m² for others. Contract: Contract number for aerial photos or for
 906 scanning report. BNO=Blom, T=TerraTec

| No | Name | Year | Method | A/D | Type | Res. | Contract | Date |
|-----|----------------------------|------|--------|-----|----------|------------------------|--------------|------------|
| 1,2 | Ålftobreen & Hansebreen | 1968 | aP | D | contours | 10 m | WF3210 | 1968-08-05 |
| | | 1988 | aP | D | contours | 10 m | FW9678 | 1988-09-07 |
| | | 1997 | aP | D | DTM | 10 m | FW11440 | 1997-08-14 |
| | | 2010 | aL | D | points | 0.5/m ² | T10067 | 2010-09-02 |
| 3 | Nigardsbreen | 1964 | aP | D | points | 0.2/m ² | WF1171 | 1964-09-02 |
| | | 1984 | aP | A | contours | 10 m | FW8310 | 1984-08-10 |
| | | 2009 | aL | D | points | 0.3/m ² | BNO097044 | 2009-10-17 |
| | | 2013 | aL | D | points | 1/m ² | T40235 | 2013-09-10 |
| 4 | Austdalsbreen | 1988 | aP | A | contours | 10 m | FW9659 | 1988-08-10 |
| | | 2009 | aL | D | points | 0.3/m ² | BNO097044 | 2009-10-17 |
| 5 | Rembesdalskåka | 1961 | aP | A | contours | 10 m | WF1230 | 1961-08-31 |
| | | 1995 | aP | D | contours | 20 m | FW11862 | 1995-08-31 |
| | | 2010 | aL | D | points | 0.5/m ² | T10063 | 2010-09-30 |
| 6 | Storbreen | 1968 | aP | A | contours | 10 m | WF3207 | 1968-08-27 |
| | | 1984 | aP | A | contours | 10 m | FW8336 | 1984-08-24 |
| | | 1997 | aP | D | DTM | 5 m | FW12173 | 1997-08-08 |
| | | 2009 | aL | D | points | 0.3/m ² | BNO097044 | 2009-10-17 |
| 7 | Hellstugubreen | 1968 | aP | A | contours | 10 m | WF3207 | 1968-08-27 |
| | | 1980 | aP | A | contours | 10 m | FW6555 | 1980-09-26 |
| | | 1997 | aP | D | DTM | 5 m | FW12173 | 1997-08-08 |
| | | 2009 | aL | D | points | 0.3/m ² | BNO097044 | 2009-10-17 |
| 8 | Gråsubreen | 1984 | aP | A | contours | 10 m | FW8330 | 1984-08-23 |
| | | 1997 | aP | D | DTM | 5 m | FW12173 | 1997-08-08 |
| | | 2009 | aL | D | points | 0.3/m ² | BNO097044 | 2009-10-17 |
| 9 | Engabreen | 1968 | aP | A | contours | 10 m | WF3205 | 1968-08-25 |
| | | 2001 | aL | D | points | 0.7/m ² | Topscan GmbH | 2001-09-24 |
| | | 2008 | aL | D | points | 2.6-6.0/m ² | BNO08797 | 2008-09-02 |
| 10 | Langfjordjøkelen | 1966 | aP | D | contours | 10 m | WF1800 | 1966-07-11 |
| | | 1994 | aP | D | contours | 10 m | FN94168 | 1994-08-01 |
| | | 2008 | aL | D | points | 0.6/m ² | BNO07771 | 2008-09-02 |

907

908

909 Table 3. Example of sensitivity of mass balance results of Langfjordjøkelen (1994-2008) and
 910 Storbreen (1997-2009) using area–altitude distributions from two different years, using only the first
 911 year or only the second year throughout, and homogenizing them using (1) a stepwise shift (step)
 912 halfway through the period or (2) by linearly time-weighting (linear) them. B_s , B_a are averages (m w.e.
 913 a^{-1}) for the period of record, $\sum B_a$ is the cumulative sum of B_a for the period (m w.e.).

| m w.e. | Langfjordjøkelen | | | | Storbreen | | | |
|------------|------------------|--------------|--------------|---------------|--------------|--------------|--------------|---------------|
| | only 1994 | only 2008 | (1) shift | (2) linear | only 1997 | only 2009 | (1) shift | (2) linear |
| B_w | 1.94 | 2.00 | 1.98 | 1.98 | 1.44 | 1.43 | 1.43 | 1.43 |
| B_s | -3.18 | -3.07 | -3.10 | -3.11 | -1.95 | -1.95 | -1.95 | -1.95 |
| B_a | -1.24 | -1.07 | -1.12 | -1.14 | -0.51 | -0.52 | -0.52 | -0.52 |
| $\sum B_a$ | -16.13 | -13.87 | -14.58 | -14.76 | -6.11 | -6.27 | -6.20 | -6.19 |

914

Table 4. Results of the mass balances and the uncertainty analysis for the 10 glaciers and 21 periods studied. Glacier names are shown with three characters as in Figure 1. Numbers are added for glaciers with multiple geodetic periods. B is (glaciological, geodetic and internal) mass balance and σ is the estimated random error (\pm) for the three balances. See ch. 3.4.1. for explanation of terms. All mass balances and errors are in m w.e. a⁻¹.

| No | Glacier | Period | Years | B.glac | σ .glac. | σ .glac. | σ .glac. | B. geod | σ .geod. | σ .geod. | B.int | σ .int |
|----|---------|-----------|-------|--------|-----------------|-----------------|-----------------|---------|-----------------|-----------------|-------|---------------|
| | abrev. | | | | point | spatial | ref | | DTM | dc | | |
| 1 | Ålf1 | 1968-1988 | 20 | 0.09 | 0.26 | 0.19 | 0.05 | -0.12 | 0.09 | 0.01 | -0.06 | 0.02 |
| 1 | Ålf2 | 1988-1997 | 9 | 0.99 | 0.26 | 0.19 | 0.05 | 0.87 | 0.08 | 0.05 | -0.06 | 0.02 |
| 1 | Ålf3 | 1997-2010 | 13 | -0.53 | 0.26 | 0.19 | 0.05 | -1.05 | 0.04 | 0.06 | -0.06 | 0.02 |
| 2 | Han1 | 1988-1997 | 9 | 0.07 | 0.26 | 0.19 | 0.05 | 0.61 | 0.05 | 0.04 | -0.04 | 0.01 |
| 2 | Han2 | 1997-2010 | 13 | -1.01 | 0.26 | 0.19 | 0.05 | -1.34 | 0.06 | 0.08 | -0.04 | 0.01 |
| 3 | Nig1 | 1964-1984 | 20 | 0.04 | 0.26 | 0.21 | 0.06 | 0.14 | 0.16 | 0.01 | -0.16 | 0.05 |
| 3 | Nig2 | 1984-2013 | 29 | 0.33 | 0.26 | 0.21 | 0.06 | -0.16 | 0.08 | 0.01 | -0.16 | 0.05 |
| 4 | Aus | 1988-2009 | 21 | -0.40 | 0.21 | 0.20 | 0.06 | -0.32 | 0.05 | 0.02 | -0.03 | 0.01 |
| 5 | Rem1* | 1962-1995 | 33 | 0.27 | 0.12 | 0.21 | 0.06 | 0.19 | 0.06 | 0.01 | -0.06 | 0.02 |
| 5 | Rem2 | 1995-2010 | 15 | -0.21 | 0.12 | 0.21 | 0.06 | -0.73 | 0.05 | 0.04 | -0.06 | 0.02 |
| 6 | Sto1 | 1968-1984 | 16 | -0.32 | 0.08 | 0.16 | 0.01 | -0.31 | 0.08 | 0.02 | -0.02 | 0.01 |
| 6 | Sto2 | 1984-1997 | 13 | -0.05 | 0.08 | 0.16 | 0.01 | 0.19 | 0.15 | 0.01 | -0.02 | 0.01 |
| 6 | Sto3 | 1997-2009 | 12 | -0.53 | 0.08 | 0.16 | 0.01 | -0.45 | 0.13 | 0.03 | -0.02 | 0.01 |
| 7 | Hel1 | 1968-1980 | 12 | -0.51 | 0.08 | 0.12 | 0.01 | -0.38 | 0.20 | 0.02 | -0.02 | 0.01 |
| 7 | Hel2 | 1980-1997 | 17 | -0.18 | 0.08 | 0.12 | 0.01 | -0.08 | 0.07 | 0.01 | -0.02 | 0.01 |
| 7 | Hel3 | 1997-2009 | 12 | -0.61 | 0.08 | 0.12 | 0.01 | -0.51 | 0.06 | 0.03 | -0.02 | 0.01 |
| 8 | Grå1 | 1984-1997 | 13 | -0.15 | 0.07 | 0.07 | 0.01 | -0.06 | 0.10 | 0.00 | -0.01 | 0.00 |
| 8 | Grå2 | 1997-2009 | 12 | -0.59 | 0.07 | 0.07 | 0.01 | -0.44 | 0.09 | 0.03 | -0.01 | 0.00 |
| 9 | Eng1* | 1969-2001 | 32 | 0.64 | 0.20 | 0.19 | 0.01 | -0.03 | 0.06 | 0.00 | -0.15 | 0.05 |
| 9 | Eng2 | 2001-2008 | 7 | 0.01 | 0.20 | 0.19 | 0.01 | -0.48 | 0.04 | 0.03 | -0.08 | 0.03 |
| 10 | Lan | 1994-2008 | 14 | -1.04 | 0.08 | 0.12 | 0.01 | -1.18 | 0.13 | 0.07 | -0.04 | 0.01 |

***For Eng1 and Rem1 the geodetic survey is one year before the first year of glaciological mass balance, the comparison period was adjusted to fit the glaciological measurement period.**

Table 5. Comparison of glaciological and geodetic mass balances. Δ (in m w.e. a⁻¹) is the difference over the period of record between cumulative glaciological balance and geodetic balance, corrected for internal ablation. δ (dimensionless) is the reduced discrepancy, where uncertainties are accounted for. β is the probability of accepting H0 although the results of the two methods are different at the 95 % confidence level, while ϵ (in m w.e. a⁻¹) is the limit for detection of bias. Bold is used to highlight periods with less than 10 years length, differences larger than 0.20 m w.e. a⁻¹ and reduced discrepancies larger than 1.96.

| No | Glacier | Period | Δ | δ | H0 | β | ϵ |
|----|---------|-----------|----------|----------|-----|---------|------------|
| 1 | Ålf1 | 1968-1988 | 0.15 | 1.26 | yes | 76 | 0.43 |
| 1 | Ålf2 | 1988-1997 | 0.06 | 0.43 | yes | 93 | 0.51 |
| 1 | Ålf3 | 1997-2010 | 0.46 | 3.84 | no | 3 | 0.43 |
| 2 | Han1 | 1988-1997 | -0.58 | -4.69 | no | 0 | 0.44 |
| 2 | Han2 | 1997-2010 | 0.29 | 2.14 | no | 43 | 0.49 |
| 3 | Nig1 | 1964-1984 | -0.26 | -1.41 | yes | 71 | 0.67 |
| 3 | Nig2 | 1984-2013 | 0.32 | 2.81 | no | 20 | 0.42 |
| 4 | Aus | 1988-2009 | -0.11 | -1.30 | yes | 74 | 0.3 |
| 5 | Rem1 | 1961-1995 | 0.02 | 0.27 | yes | 94 | 0.28 |
| 5 | Rem2 | 1995-2010 | 0.45 | 4.85 | no | 0 | 0.34 |
| 6 | Sto1 | 1968-1984 | -0.02 | -0.26 | yes | 94 | 0.33 |
| 6 | Sto2 | 1984-1997 | -0.26 | -1.70 | yes | 60 | 0.56 |
| 6 | Sto3 | 1997-2009 | -0.11 | -0.76 | yes | 88 | 0.52 |
| 7 | Hel1 | 1968-1980 | -0.15 | -0.74 | yes | 89 | 0.73 |
| 7 | Hel2 | 1980-1997 | -0.12 | -1.51 | yes | 67 | 0.28 |
| 7 | Hel3 | 1997-2009 | -0.12 | -1.44 | yes | 70 | 0.29 |
| 8 | Grå1 | 1984-1997 | -0.10 | -0.91 | yes | 85 | 0.37 |
| 8 | Grå2 | 1997-2009 | -0.16 | -1.59 | yes | 64 | 0.37 |
| 9 | Eng1 | 1969-2001 | 0.52 | 5.54 | no | 0 | 0.34 |
| 9 | Eng2 | 2001-2008 | 0.41 | 3.53 | no | 6 | 0.42 |
| 10 | Lan | 1994-2008 | 0.10 | 0.67 | yes | 90 | 0.56 |

Figures

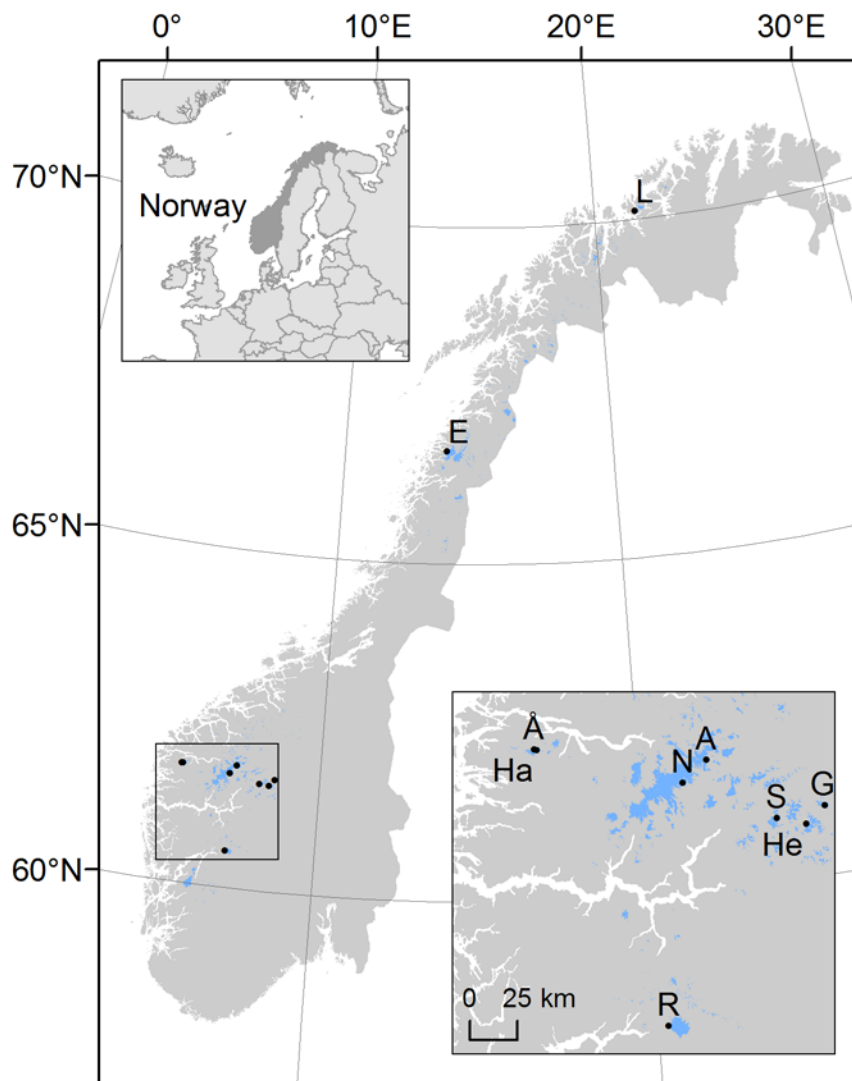


Figure 1. Location map of Norway showing the ten study glaciers with long-term glaciological mass balance series. Glaciers are shaded in blue. See Table 1 for details on the glaciers. The inset shows Norway's location in Europe and a zoom in on the eight glaciers in southern Norway.

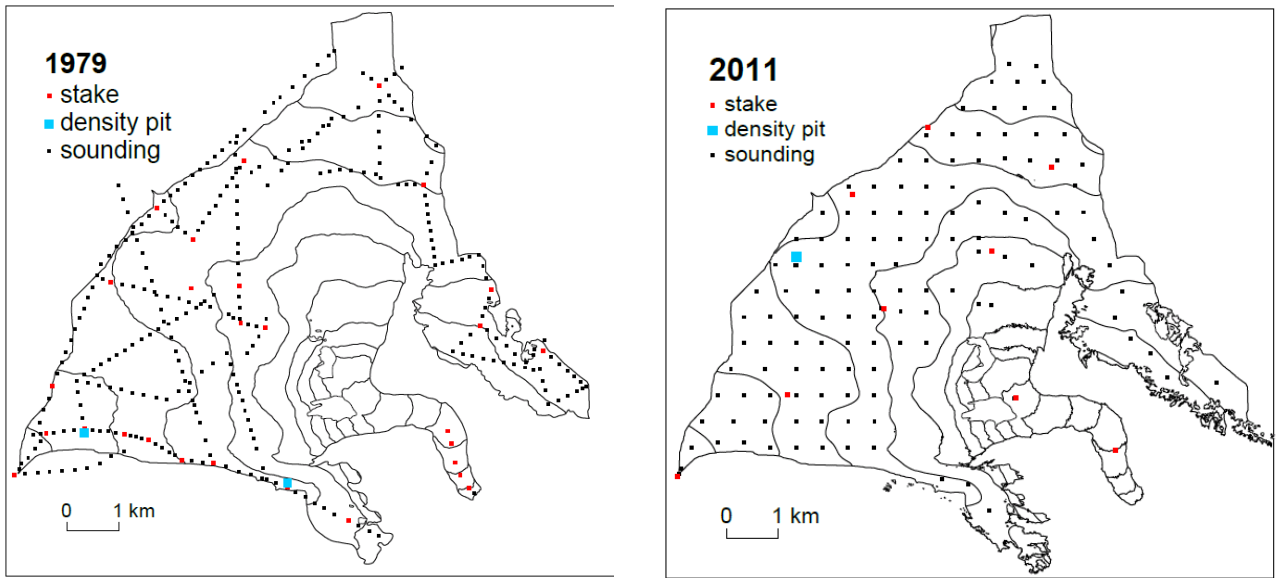


Figure 2. Typical stake network and snow depth soundings for Nigardsbreen. Non-glaciated areas within the basin are shaded in grey. The network in 1979 is representative for the period 1962-81, whereas 2011 is representative for 2009-2014. The glacier outlines are from 1974 and 2013, respectively.

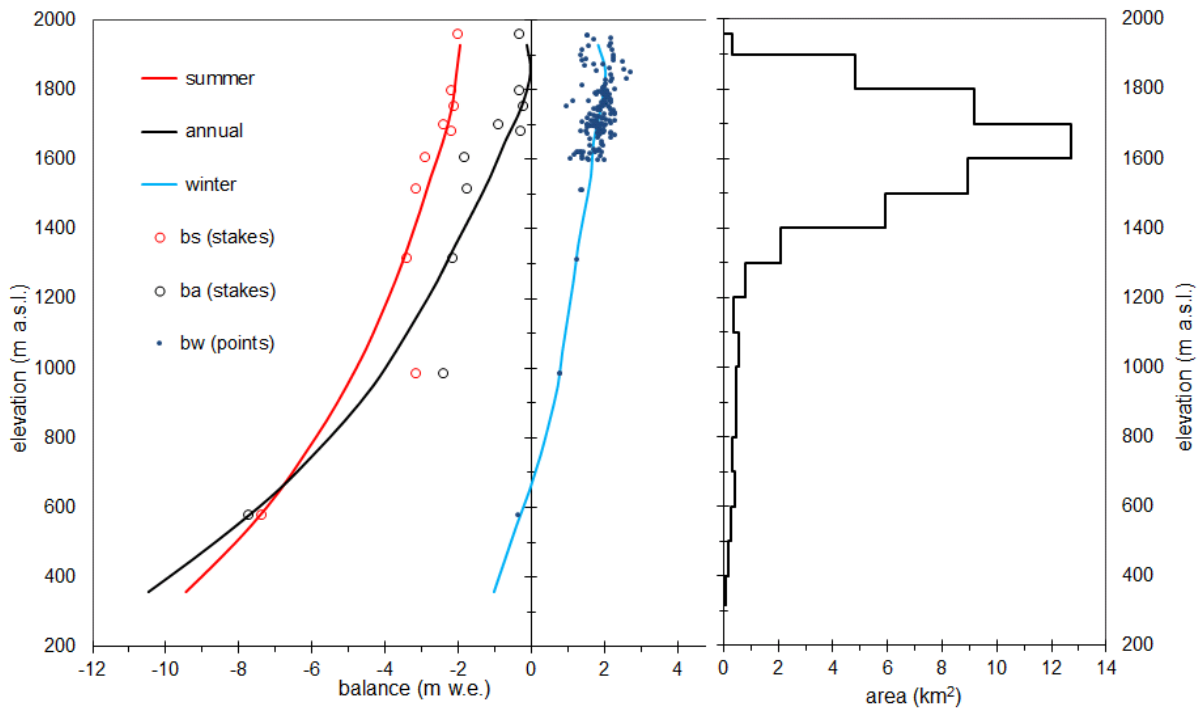


Figure 3. Illustration of the profile method for Nigardsbreen 2003. The altitudinal winter, summer and annual mass balance curves and point values for b_w (\square), b_s (\circ) and b_a (\bullet), together with average b_w (\square) for each 100 m altitude interval are plotted versus altitude.

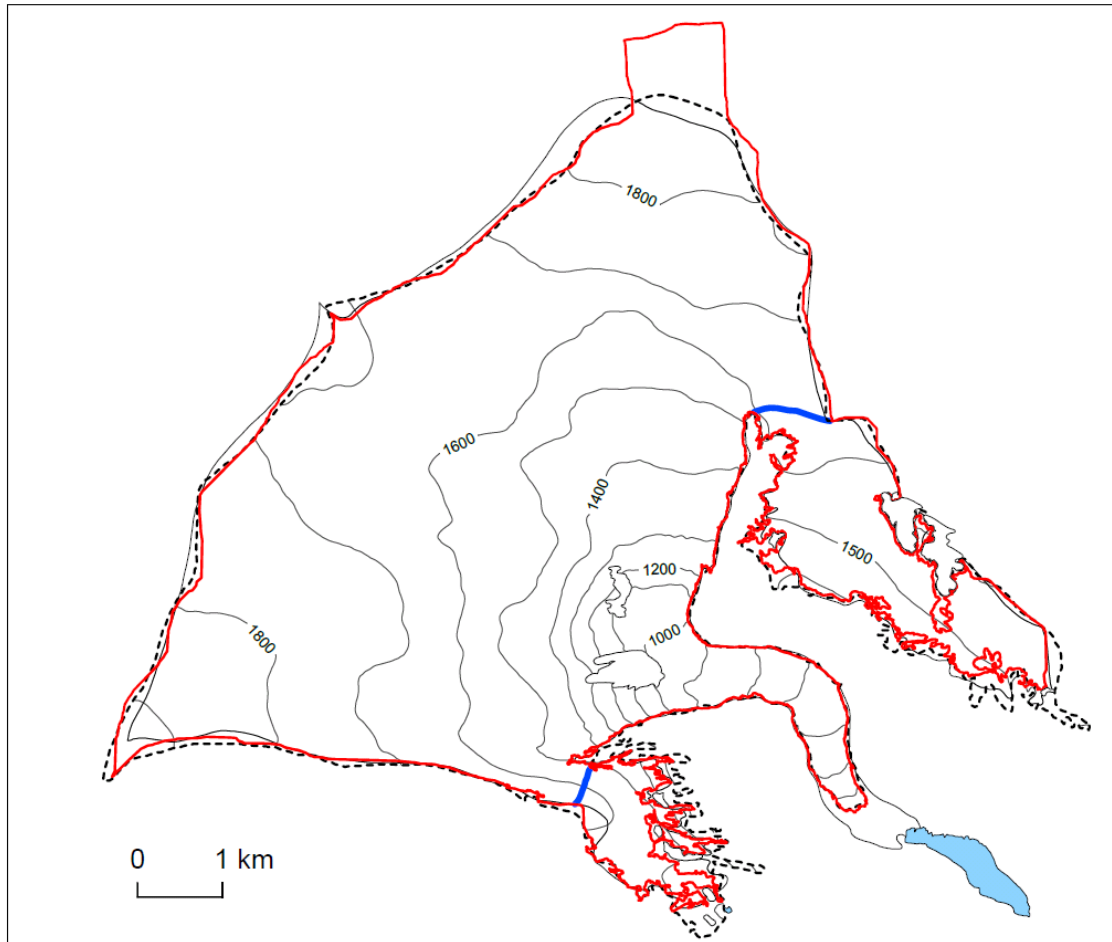


Figure 4. The hydrological basins of Nigardsbreen. The basin derived from the 2013 mapping in red, dotted line shows the 1984 extent and basin, black solid line shows the 1964 extent. The glaciological divide used in the first years are marked in blue. Elevation contours are 100 m derived from the 2013 DTM. Lake Nigardsbrevatn are shaded in turquoise.

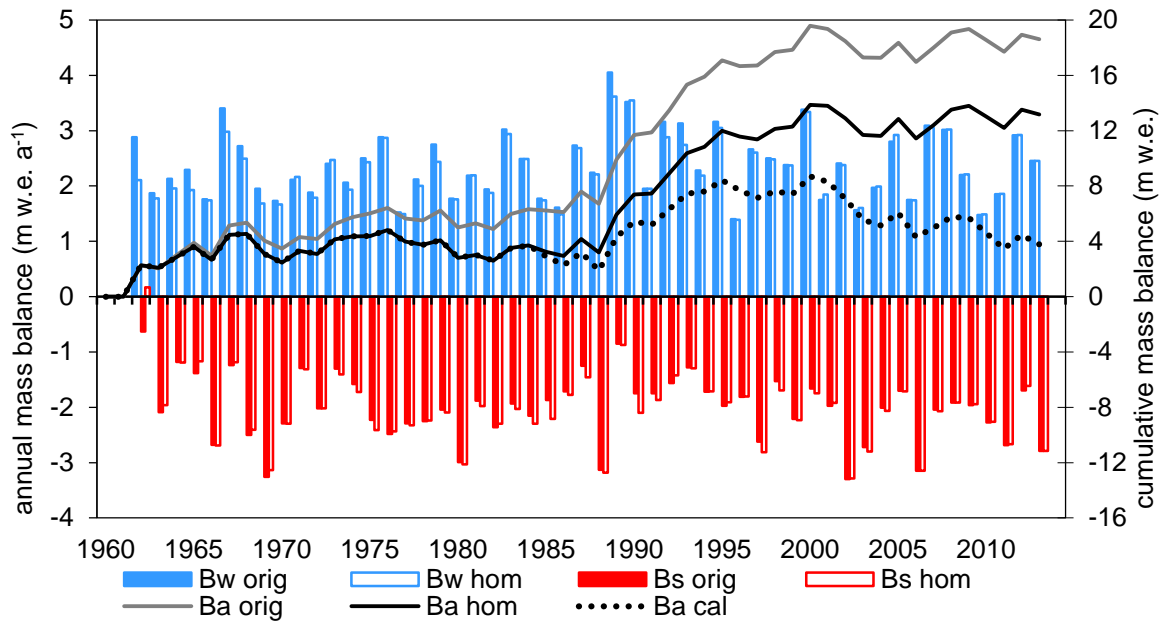


Figure 5. Original, homogenized and calibrated mass balance series for Nigardsbreen. Annual values are shown for Bw and Bs and cumulative values are shown for Ba. See supplementary table S1 for individual values.

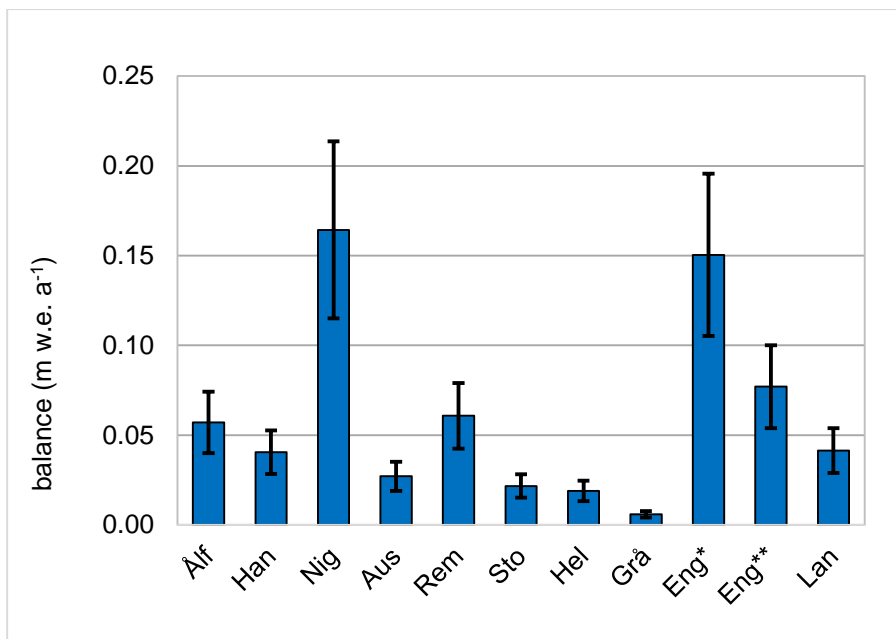


Figure 6. Calculated internal ablation for the ten study glaciers. The values are the the annual mean for the reference period 1989-2013. Calculations are divided in two periods for Engabreen, *1989-1992 and **1993-2013, since the subglacial water was captured by a tunnel under the glacier from 1993. Error bars are 1/3 of the calculated value.

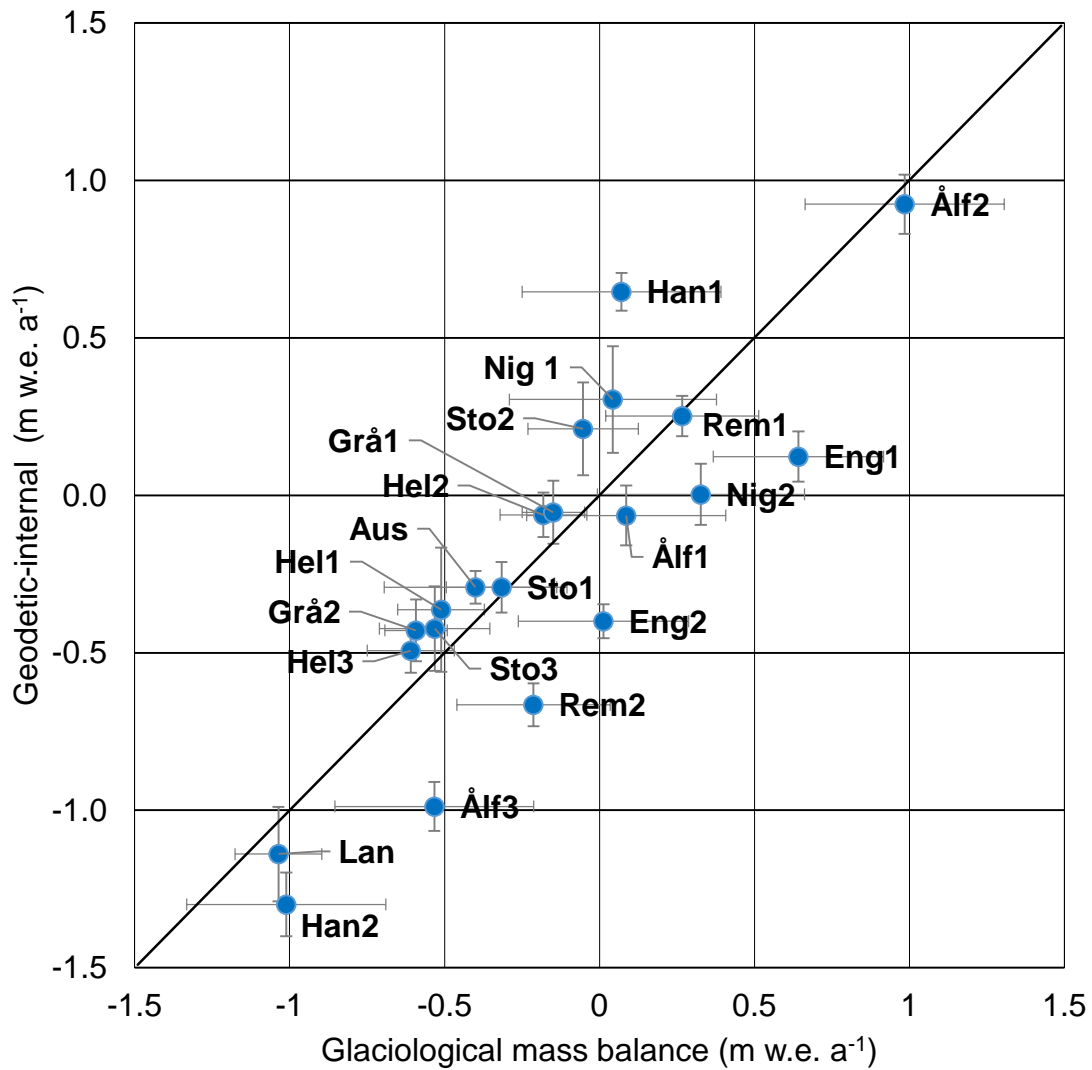


Figure 7. Glaciological versus geodetic mass balance, subtracting the calculated internal mass balance from the geodetic balance, with error bars for glaciological and geodetic. Glacier names are shown with three characters as in Figure 1. Numbers are added for glaciers with multiple geodetic periods, e.g. Eng1 refers to the first geodetic period and Eng2 to the second period for Engabreen.

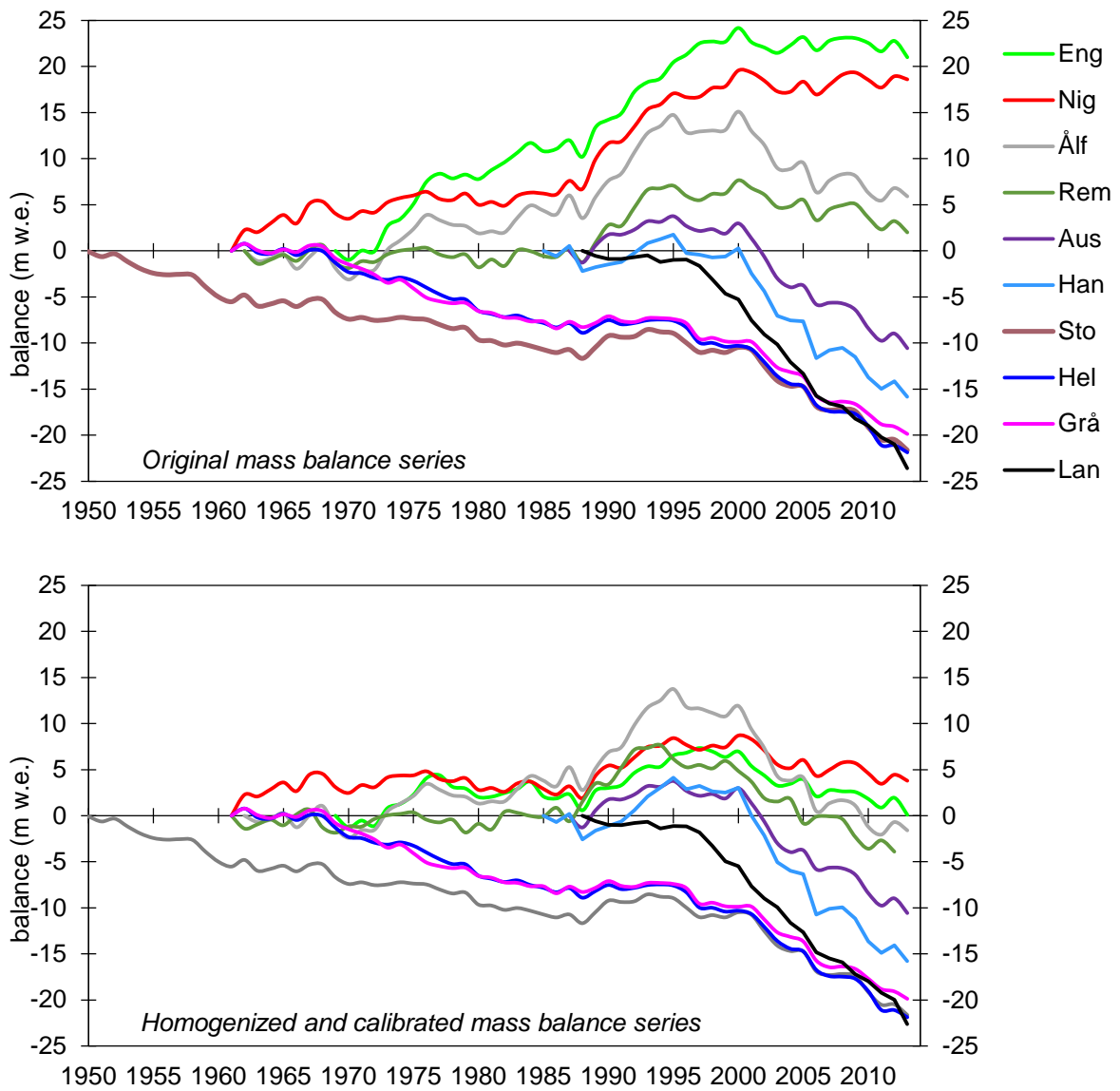


Figure 8. Cumulative glaciological mass balances for the 10 long term glaciers. Upper diagram shows original series prior to homogenization. Lower diagram shows homogenized and partly calibrated series. Calibration was applied to Nigardsbreen (1984-2013), Hansebreen (1988-2010), Ålfotbreen (1997-2010), Rembesdalskåka (1995-2010) and Engabreen (1970-2008).